Active and Adaptive Damping of Chatter Vibrations in the Boring Process using Magnetorheological Damper

by

Mostafa Khalil Abdou Saleh

A Dissertation Submitted to the
Graduate School of Sciences and Engineering
in Partial Fulfillment of the Requirements for
the Degree of

Doctor of Philosophy

in

Mechanical Engineering

KOÇ ÜNİVERSİTESİ

6 August 2021

Active and Adaptive Damping of Chatter Vibrations in the Boring Process using Magnetorheological Damper

Koç University

Graduate School of Sciences and Engineering

This is to certify that I have examined this copy of a doctoral dissertation by

Mostafa Khalil Abdou Saleh

and have found that it is complete and satisfactory in all respects,

and that any and all revisions required by the final

examining committee have been made.

Committee Members:

Prof. İsmail Lazoğlu (Advisor)

Assoc. Prof. Arif Karabeyoğlu

Prof. Funda Acar Yağcı

Prof. Erhan Budak

Prof. Mustafa Bakkal

Date: 06.08.2021

To my mother, my wife, and my little princess Mawadda

ABSTRACT

Active and Adaptive Damping of Chatter Vibrations in the Boring Process using Magnetorheological Damper

Mostafa Khalil Abdou Saleh
Doctor of Philosophy in Mechanical Engineering
6 August 2021

Chatter is a limiting factor during boring of deep holes with long slender boring bars. This thesis introduces a new magnetorheological (MR) damper to suppress the chatter and increase the stability of the boring process. A novel design that utilizes a minimal amount of MR fluid filled in a sponge layer surrounding the boring bar is presented. The MR fluid layer and the electromagnetic circuit are externally applied to the boring bar, which allows easy installation and adjustability of the overhang length of the bar. A custom made, bidisperse MR fluid which has an improved sedimentation resistance property is used to ensure a long lifetime of the damper.

A new sliding mode control with variable gain super twisting algorithm is designed and implemented for active damping of chatter vibrations in the boring process using the developed MR damper. Simulations of the controller show its fast response and robustness against disturbances and parameters uncertainties. The proposed controller outperforms the commonly used PID controller for disturbance rejection at wide range of frequencies.

Experimental validations of the developed system were performed on CNC turning center. The modal analysis of the boring bar with the new MR damper shows improvements in both the damping and the dynamic stiffness of the system. This enhancement significantly increases the chatter-free depth of cut on the stability lobe diagrams. Validation cutting tests were performed under various machining conditions on boring of Al7075 and Inconel 718 workpieces which are materials widely used in many aerospace applications. The improvements achieved by this work are illustrated in terms of measured acceleration values in both time and frequency domains, in addition to the quality of the machined surfaces.

ÖZETÇE

Manyetoreolojik Amortisör Kullanarak Borlama Sürecindeki Tırlama Titreşimlerinin Aktif ve Adaptif Olarak Sönümlemesi

Mostafa Khalil Abdou Saleh
Makine Mühendisliği, Doktora
6 Ağustos 2021

Tırlama, uzun ve ince katerler ile derin deliklerin delinmesi işleminde sınırlayıcı bir faktördür. Bu tez, delme işleminin stabilitesini arttırmak ve tırlamayı sönümlemek için yeni bir manyetoreolojik (MR) damperi tanıtmaktadır. Kateri çevreleyen bir sünger tabakasına doldurulmuş minimum miktarda MR sıvısı kullanan yeni bir tasarım sunulmaktadır. MR sıvı tabakası ve elektromanyetik devre, kolay kurulum şansı sağlayıp overhang uzunluğunun ayarlanabilmesini sağladığından katere harici olarak uygulanmaktadır. Damperin uzun ömürlü olmasını sağlamak için geliştirilmiş, çökme/tortulaşma direncine sahip özel yapım iki dağılımlı bir MR sıvısı kullanılmıştır.

Geliştirilen MR sönümleyici kullanılarak delme işleminde tırlama titreşimlerinin aktif sönümlenmesi için değişken kazançlı super-twisting algoritmalı yeni bir kayan mod kontrolü tasarlanmış ve uygulanmıştır. Kontrolörün simülasyonları, dış bozucu etkilere ve parametrik belirsizliklere karşı hızlı tepkisini ve sağlamlığını göstermiştir. Önerilen denetleyici, geniş frekans aralığında yaygın olarak kullanılan PID denetleyicisinden daha iyi performans göstermektedir.

Geliştirilen sistemin deneysel doğrulamaları CNC torna tezgahında yapılmıştır. Yeni MR sönümleyici kullanılan katerin modal analizi, sistemin hem sönümlemesinde hem de dinamik rijitliğinde iyileştirmeler göstermiştir. Bu geliştirme, stabilite lob diyagramlarında titreşim oluşmadan kullanılabilecek kesme derinliğini önemli ölçüde arttırmaktadır. Birçok havacılık uygulamasında yaygın olarak kullanılan malzemeler olan Al7075 ve Inconel 718 iş parçalarının delinmesi için çeşitli kesme koşulları altında doğrulama kesme testleri yapılmıştır. Bu çalışma ile elde edilen iyileştirmeler, işlenmiş yüzeylerin kalitesine ek olarak hem zaman hem de frekans alanlarında ölçülen ivme değerleri ile gösterilmektedir.

ACKNOWLEDGMENTS

I would like to express my sincere gratitude to my thesis advisor Professor Ismail Lazoğlu for his guidance, patience, and continuous help throughout my PhD. I am really grateful to him for giving me the opportunity to work in such dynamic research environment at the Manufacturing and Automation Research Center (MARC), where I gained a lot of experiences that will shape my future. I am also very thankful to Professor Funda Acar Yağcı and Professor Arif Karabeyoğlu for their time and constructive comments during the periodic research meetings. I also wish to express my sincere appreciation to Professor Erhan Budak and Professor Mustafa Bakkal for being in my thesis committee.

I would like to acknowledge the kind support of Koç university, the Scientific and Technological Research Council of Turkey (TÜBITAK), Arçelik A.Ş., Alp Aviation Inc., and Sandvik Coromant to accomplish this research.

I am also very thankful to my research partner Abasin Ulasyar as we spent long time working side by side on different phases of the project. I have learned a lot of things from him. I would like to thank professor Funda once again, and her student Mona Nejatpour for supporting us with the distinguished MR fluid which they developed and delivered to us whenever was needed. I would like to express my appreciation to our lab technician Muzaffer Butun, and all my friends and colleagues in MARC where we shared a lot of memorable time that has become a notable experience in my personal and professional development.

Finally, I wish to express my deepest gratitude to my family for their love, patience, and unlimited support. No words can properly describe my feelings towards them. I dedicate this work to them.

TABLE OF CONTENTS

LIST OF TABLES

LIST OF FIGURES

ABBREVIATIONS

CNC	Computerized Numerically Controlled
FEM	Finite Element Modeling
FRF	Frequency Response Function
MR	Magnetorheological
MRF	Magnetorheological Fluid
PID	Proportional-Integral-Derivative
SMC	Sliding Mode Control
VGSTA	Variable Gain Super-Twisting Algorithm

Chapter 1

INTRODUCTION

1.1 Overview

Boring process is one of machining operations which is performed to enlarge the inner diameter of premanufactured holes. In this process, a single point cutting tool is usually used for continuous removal the material from the internal walls of the rotating workpiece. Long slender bars with high length to diameter ratios are used for boring of deep holes. These bars have low stiffness due to the cantilever structure configuration of the boring process, as shown in Figure 1.1, which makes the system prone to high possibility of chatter vibrations. Chatter affects the quality of machined surfaces, leads to excessive forces and vibrations, and may cause damage on cutting inserts, parts, and machine tools which interrupts the manufacturing process and adds unexpected cost to the manufactured parts. Damping of these undesired vibrations has been considered as an important topic for machining industry for decades.

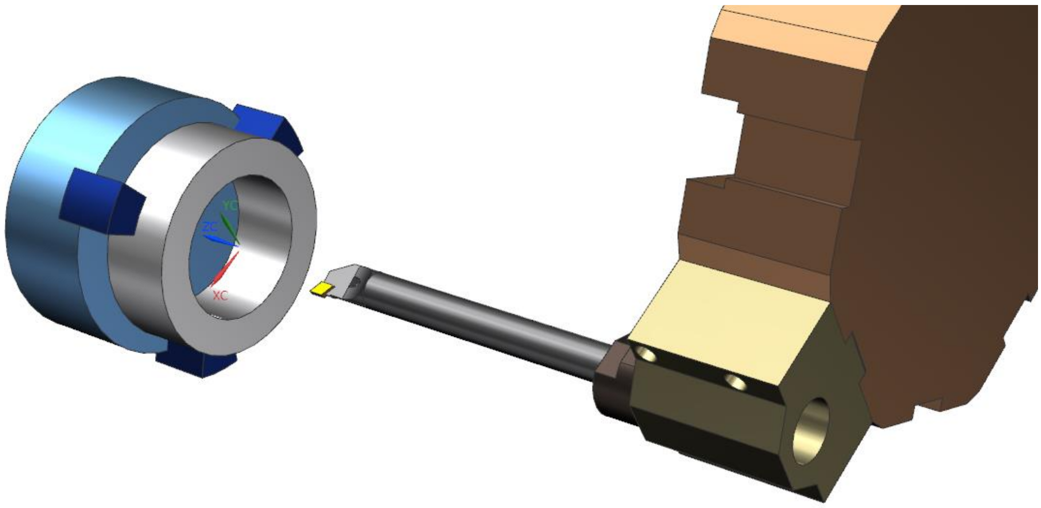

Figure 1.1: Schematic diagram of the boring process setup on turning center.

1.2 Passive and active solutions

Different active and passive techniques have been used to overcome this problem. Passive techniques have the advantages of simplicity in installation and maintenance, relatively low cost, and no external power requirement; however, they have some limitations regarding the working bandwidth as they have fixed design parameters that cannot be altered after manufacturing. For these reasons, the effectiveness of passive dampers is reduced in case of machining under variable cutting conditions. In contrast, active techniques can damp different chatter modes. Active devices require an external power source to adjust the applied damping according to the required modes. They are integrated with sensors in a closed-loop control system for online chatter control. The continuous adjustment of damping or stiffness allows real-time adaptive chatter suppression. Different active damping techniques have been used for the boring process including piezoelectric elements, magnetic and electromagnetic actuators, electrorheological and magnetorheological fluid devices. Some of these active techniques are used without a feedback loop in a semi-active mode, which indicates a manual interference for tuning of the damping properties during the operation. Semi-active chatter suppression has better damping properties than passive ones, while having lower power consumption, simpler control circuit, and lower cost than active suppression. However, active techniques are the best option for complete automated process that is a key factor in next generation smart manufacturing facilities.

1.3 Magnetorheological fluid dampers

Magnetorheological (MR) fluids are field-dependent, non-Newtonian fluids, which consist of micron-sized ferrous particles suspended in a carrier fluid. The rheological properties like viscosity and yield stress of the fluid are controlled by varying the magnetic flux intensity. The change in these properties is controllable and completely reversible when releasing the activation field (Carlson and Jolly, 2000). Due to these unique properties, MR fluids are used in active and semi-active vibration suppression devices for several mechanical and civil engineering applications (Zhu et al., 2012). Moreover, in machining field, MR fluids were used for various purposes, including flexible mounts, surface finishing of free form surfaces, and damping of chatter vibrations in boring, turning, and drilling operations (Lu et al., 2021).

1.4 Research Objectives

This thesis aims to provide an active damping device for chatter suppression in the boring process. A novel sponge-type MR fluid damper is designed and manufactured. The damper is designed in cylindrical shape so that it provides damping in all radial directions of the bar. The proposed sponge-type configuration reduces the required amount of MR fluid in addition to eliminating the need of tight sealing. The damper can be easily installed on CNC turning centers and can be used with commercial boring bars without modifications by wrapping the MR sponge layer outside the boring bar and activating it by the external electromagnetic circuit. Moreover, the overhang length can be adjusted according to the process requirements.

The MR fluid which is used in this study is custom made bidisperse magnetorheological fluid (MRF), composed of micro and nano-sized magnetizable particles. This fluid has high yield strength and better sedimentation resistance compared to commercial MR fluids. The linear range of the magnetic properties of the MRF is considered to avoid magnetic saturation and to eliminate nonlinearity constraints in the controller design.

In addition to the damper design, a new sliding mode controller based on variable gains super twisting algorithm is presented for the boring bar with the MR damper. The developed controller allows for compensation of unmodelled dynamics and parameter uncertainties. It shows strong robustness against disturbances in wide range of frequencies when compared to PID controller.

The developed MR damping system is successfully tested on boring of Inconel 718 and Al7075 workpieces under various cutting conditions. Orthogonal calibration tests were performed on the two materials to obtain the cutting coefficients. The frequency response function (FRF) obtained from the impact tests shows significant improvements in the damping and dynamic stiffness of the new system. Stability lobe diagrams were generated, showing a notable increase in the chatter-free depth of cut.

Chapter 2

LITERATURE REVIEW

2.1 Overview

Chatter in the boring process is a well-known problem in machining industry. Researchers have been developing various solutions to overcome this problem with efficient and sustainable techniques. In this chapter, several articles regarding this topic were reviewed and explained. The reviewing process covered the following points: dynamics of boring process, boring bar chatter, passive and active damping techniques, and most specifically magnetorheological dampers and their applications in the boring process. Based on the reviewed literature, the research directions are highlighted at the end of the chapter.

2.2 Dynamics of boring process

Studying the dynamics of the boring process is essential to understand the cutting forces, tool-chip interaction, and chatter dynamics. Cutting forces are dependent on chip load which is function of insert geometrical parameters such as nose radius and inclination angle in addition to machining conditions like radial depth of cut and feedrate. Atabey et al. (2003) introduced a mechanistic model in addition to analytical model based on orthogonal to oblique transformation to estimate the cutting forces in the three perpendicular directions.

Lazoglu et al. (2002) developed a time-domain model that is numerically solved to predict instantaneous cutting forces and vibrations during boring operation. It can estimate the topography of the machined surface, considering the cutting process parameters, and geometries of both tool and workpiece. Simulations results were experimentally validated for various machining conditions. They showed that boring bar vibrates in radial and tangential directions while it is more rigid in the axial direction; however, the dynamic chip load is highly affected by radial vibrations rather than tangential vibrations as illustrated in Figure 2.1.

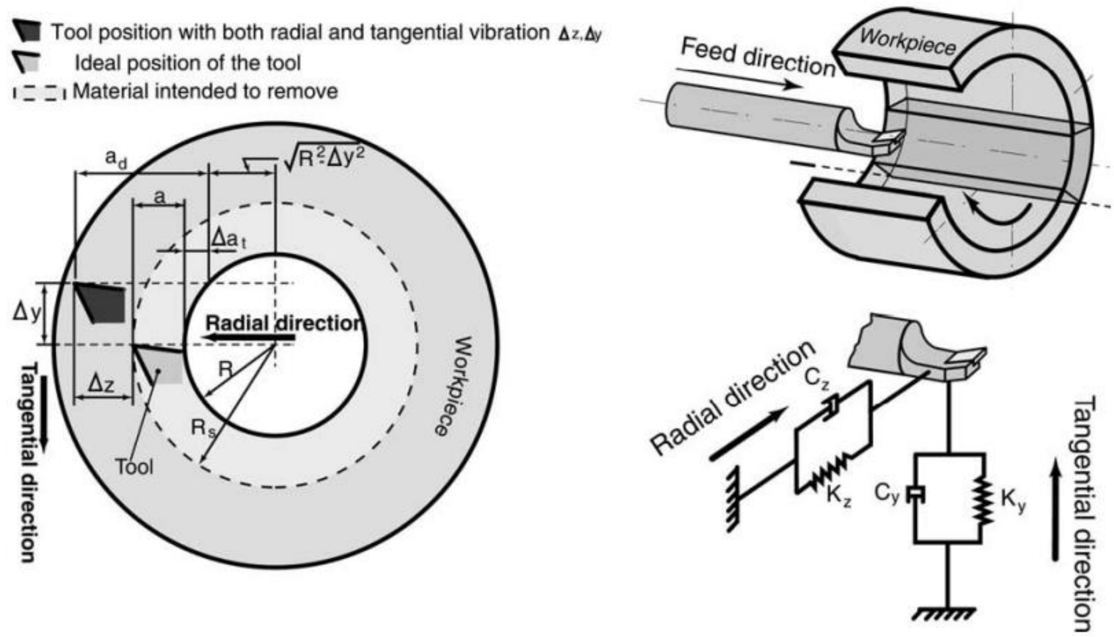

Figure 2.1: Effect of radial and tangential vibrations on chip thickness (Lazoglu et al., 2002).

Another approach for estimating the dynamic cutting forces during boring operation was given by Imani and Yussefian (2009). In their model, a geometrical approach based on B-spline is proposed for tool-workpiece interaction. In addition to estimating cutting forces, the model is used for chatter detection during boring process. The model is experimentally validated for force estimation within 15% error. The proposed geometrical approach combines the flat and curved parts of cutting edge to be used for both finishing operation when the depth of cut is less than insert nose radius and during roughing operation when vice versa. Although, Euler-Bernoulli beam theory is used in their model, they mentioned that practically it is overestimating the first natural frequency; thus, it should be found experimentally using impact hammer test.

Variation in dynamic chip loading during boring operation leads to continuous change in dynamic cutting force which consequently affect the chip thickness again in an iterative manner. This is a well-known phenomenon in metal cutting that is expressed as self-excited or chatter vibrations. Figure 2.2 explains the regenerative chatter mechanism due to phase delay between two successive cutting paths.

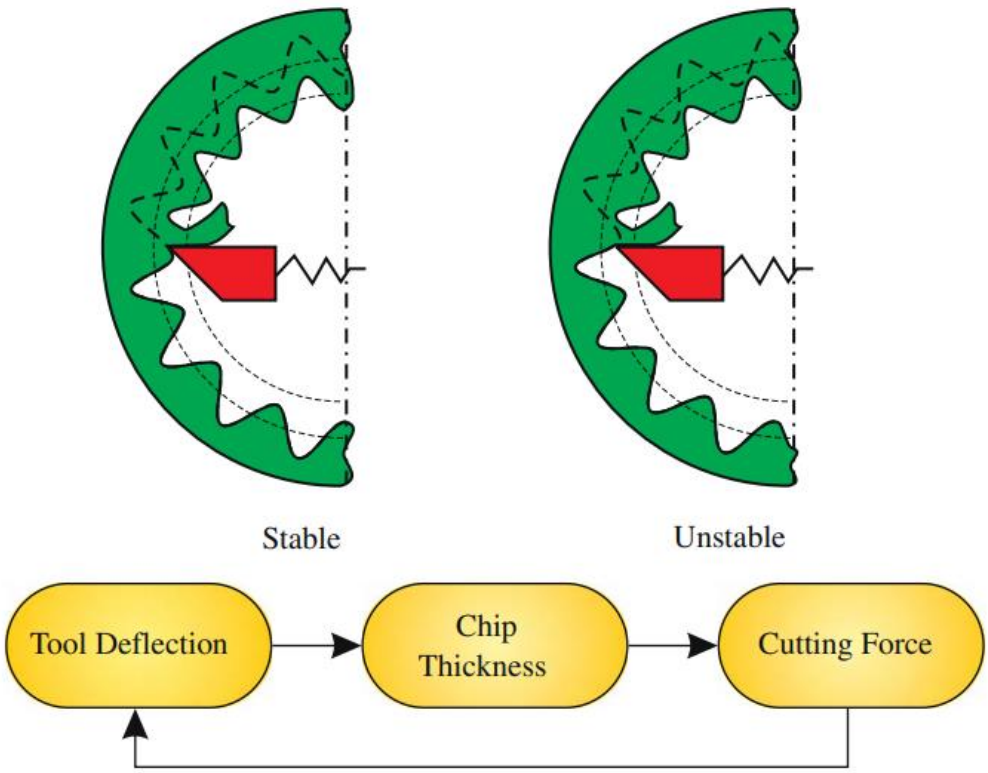

Figure 2.2: Mechanism of regenerative chatter in boring process (Moetakef-Imani and Yussefian, 2009).

Chatter in machining operations can be predicted and stability limit of allowable depth of cut is plotted against spindle rotating speed on stability lobe diagrams as shown in Figure 2.3. It has been reported by many researchers as stability criteria for different machining operations. The basic model for stability lobe prediction was introduced by Tlusty and Polacek (1963) for orthogonal turning. Frequency response function FRF of the structure is found experimentally, then it is scanned in an iterative loop to plot the absolute stable depth of cut at each frequency (Altintas, 2012). The same approach is reported for milling operation by employing the Fourier expansion to approximate the dynamic cutting force coefficients, in addition to including the effects of number of teeth, radial depth of cut, and entry and exit angles (Altintaş and Budak, 1995).

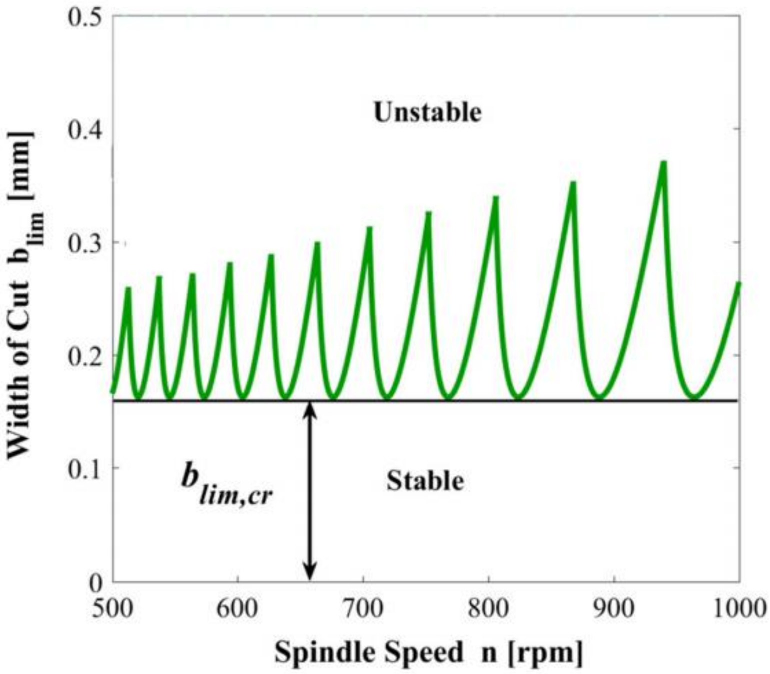

Figure 2.3: Example of stability lobe diagrams for boring process (Fallah and Moetakef-imani, 2019).

In turning and boring operations, where a single point continuous cut is considered and due to low spindle speed, other factors should be considered for accurate prediction of stability limits. Since the insert nose radius is relatively large as compared to the radial depth of cut, especially during finishing operations, Ozlu and Budak (2007) developed an elaborated model to find the stability limit of turning and boring operations within the nose radius. The cutting edge of the insert is discretized in the nose radius contact region, and the stability limit is searched step by step for every segment of the nose radius. They showed that the stability limit is drastically decreased by increasing the insert nose radius. They provided experimental validations for both turning and boring operations. It is concluded from their work that large nose radius drastically reduces stability limit for boring process (Ozlu and Budak, 2007b).

In addition to nose radius effect, the stability limits are highly affected by the contact between the machined surface and the flank surface of the tool, especially at low spindle speeds. This phenomenon is known as process damping effect which results in higher stability limits at low spindle speeds (Eynian and Altintas, 2009).

2.3 Passive damping techniques

Passive damping techniques for chatter vibrations rely on permanent modifications to the boring bar that dissipate vibration energy and enhance stability of the system. In some approaches, layers of damping materials are added to the boring bar to have an increased stiffness or damping that improves vibration resistance. The second classical approach is to use an additional spring-mass-damper subsystem as dynamic vibration absorber or tuned mass damper. There are also other techniques such as impact dampers, particle dampers, and frictional dampers. Some techniques are based on structural modifications like creating some notches on the shank on the bar.

2.3.1 Damping layers

Prasannavenkadesan et al., (2015) attached a layer of brass to conventional boring bar and investigated its effect on displacement of the bar and cutting temperature. Another boring bar with constrained layer damping is introduced by Song et al., (2016). As shown in Figure 2.4, a layer of viscoelastic damping material is attached to the main substrate layer of the boring bar and covered by the outer constrained layer. They proposed analytical and FEM optimization techniques to find the optimal diameter values of the layers to maximize the loss factor. Improvements on the modal parameters and experimental cutting tests were addressed. The stability of boring process is improved five times using the proposed damped bar.

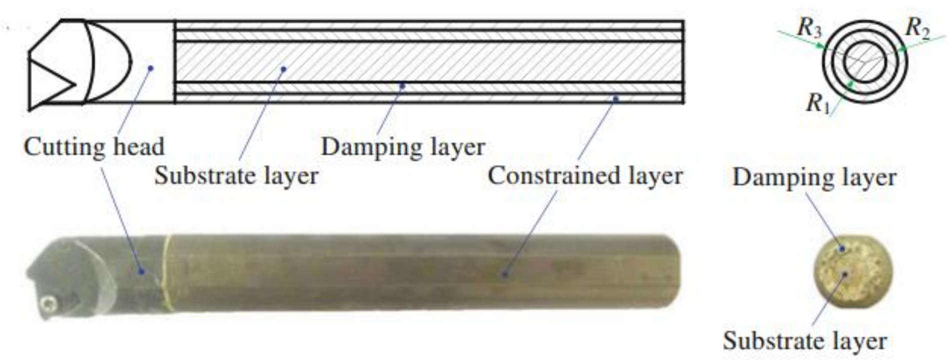

Figure 2.4: Boring bar with constrained layer damping (Song et al., 2016).

2.3.2 Impact and Particle dampers

Another old passive approach is impact or acceleration damper, in which a single additional mass is placed in a cavity used to eliminate undesirable vibration in mechanical system. This damper is relatively cheap, simple in construction and has good damping performance over different accelerations and frequencies (Lawrance et al., 2019). Similar approach that utilizes some metal particles in the axial groove of the boring bar is known as particle damped bar. Suyama et al., (2016) introduced a particle-damped boring bar, in which a steel bar is axially drilled and partially filled with 0.5-1.0 mm diameter steel particles as shown in Figure 2.5. Similar approach with relatively bigger metal spheres is proposed by (Thomas et al., 2019).

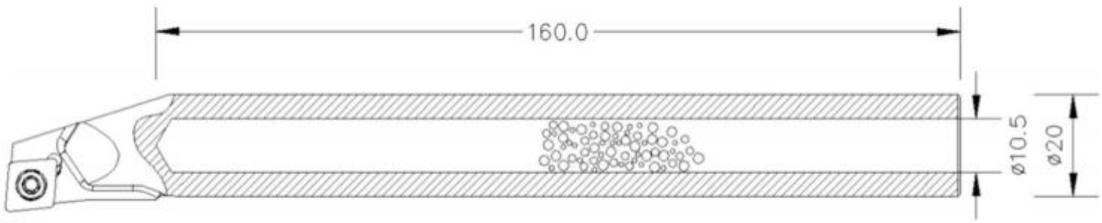

Figure 2.5: Particle-damped boring bar (Suyama et al., 2016).

2.3.3 Structural modifications

Modifying the shape of the bar for better stability is another passive technique to design more stable boing tools. Recently, Takahashi et al. (2021) introduced a new boring tool with anisotropic structure to increase the dynamic stiffness and improve chatter stability of boring process. The proposed anisotropic boring bar with tapered horn and notches is shown in Figure 2.6. They proposed FEM design method to designed and analyze the natural frequency and compliance of the new boring tool. Two boring bars with different length to diameter ratios of 4 and 10 were designed using the proposed method. Experimental verifications are not included in this work. Another tunable passive boring bar that makes use of the axial groove is achieved by inserting a long steel bolt in a threaded axial hole in the boring bar. The natural frequency is varied by adjusting the empty space of the threaded cavity (Hayati et al., 2018).

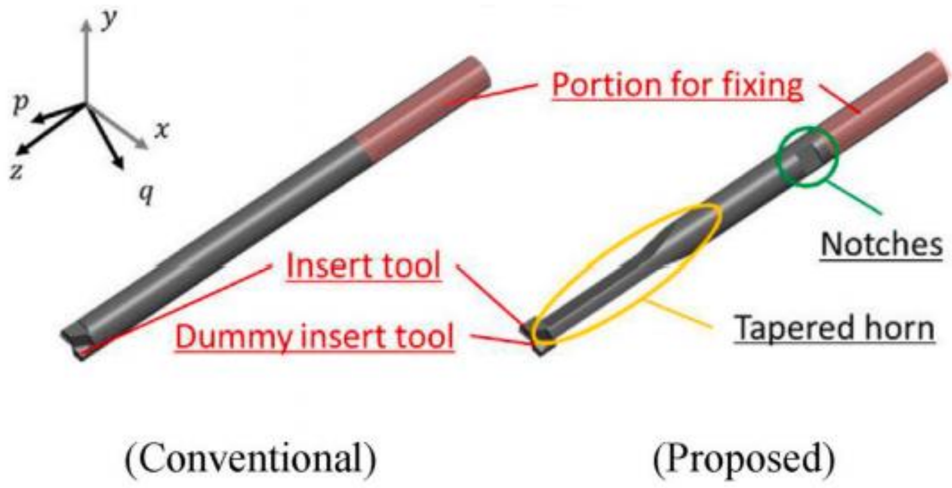

Figure 2.6: Conventional and the proposed anisotropic boring bars (Takahashi et al., 2021).

2.3.4 Dynamic vibration absorber

Dynamic vibration absorber (DVA) is a successful passive technique that has been implemented and commercialized for long boring tools. Its theory depends on adding an extra subsystem of spring-mass-damper to the boring bar. By this method, the vibrations of the structure are transferred to the subsystem leaving the tip of the boring bar with minimal displacement. (Miguélez et al., 2010) introduced two different approaches for tuning absorber parameters to achieve higher depth od cut on stability lobe diagrams. More stability analysis of passively damped boring bar with dynamic absorber is studied by Fallah and Moetakef-Imani, (2017) they showed that dynamic absorber considerably increases the stability limits of the boring process.

The main challenge of this method is the tuning of the absorber parameters which must be accurately tuned to get the desired performance otherwise it loses its effectiveness when deviated from the desired values. The other problem is to manufacture the absorber inside the boring bar as it cannot be externally applied because it must be very close to the tip.

Generally, passively damped boring bars showed good performance in reducing chatter vibrations at relatively low cost without need of additional complex components; however, they are limited to specific cutting conditions and working bandwidth. Moreover, they cannot deal with unexpected vibrations that might happen due to several reasons during metal cutting.

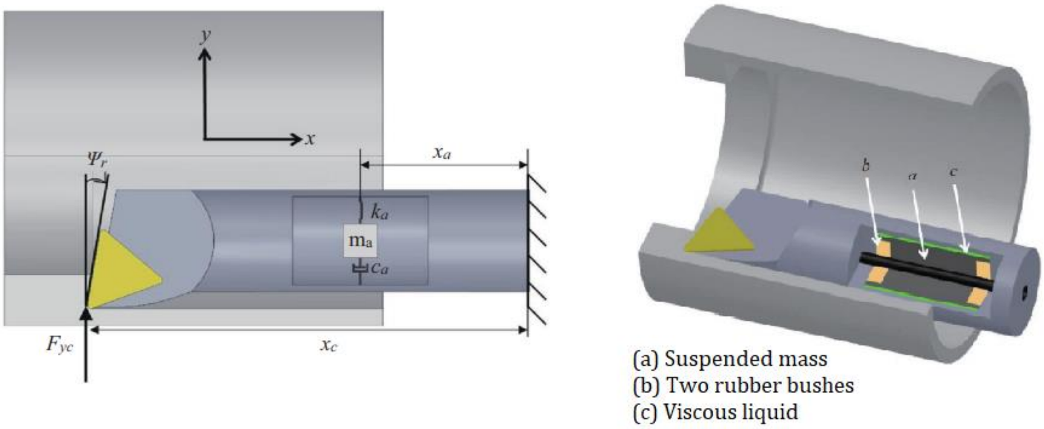

Figure 2.7: Schematic and CAD model of boring bar with dynamic vibration absorber (Fallah and Moetakef-Imani, 2017).

2.4 Active damping techniques

Active damping techniques have great potential in improving stability of boring bars. Unlike passive techniques, active dampers can suppress vibrations in a wide range of frequencies. Different techniques have been reported for active damping of boring bars including piezoelectric devices, electromagnetic actuators, and magnetorheological fluids.

2.4.1 Piezoelectric devices

Piezoelectric elements have been used for both passive and active damping of boring bars in several works. Matsubara et al., (2014) developed an equivalent dynamic absorber using a piezoelectric actuator embedded in the boring bar with an inductance-resistance circuit. Venter et al., (2017) studied active and passive damping of boring bars by attaching piezoelectric sheets to the boring bar with a passive shunt circuit. They integrated it with velocity feedback for active mode, which showed more robustness than the passive one. Yigit et al., (2017) used analytical and numerical optimization for piezoelectric shunt circuit parameters. While piezoelectric devices were successfully tested in different operations, they have limitations regarding hysteresis and complexity of installation.

2.4.2 Magnetic actuators

Magnetic and electromagnetic devices are used for active damping in different forms. Chen et al., (2014) introduced a non-contact magnetic actuator for boring bars. Their approach increases stiffness and damping in the radial and tangential directions, in addition to the torsional direction of the boring bar. It is integrated with a fiber optic sensor in a closed-loop control system (Lu et al., 2014). Their system can damp the required chatter mode with a linearized magnetic circuit. As shown in Figure 2.8, the size of the system is relatively big and bulky considering the limited space in turning machines.

Another application for active damping is given by Abele et al., (2016) who integrated an electromagnetic inertial mass damper into a boring bar, accompanying it with the required electronic circuit components as shown in Figure 2.9. The bar was specially designed with three different modules that are connected to each other which adds complexity for design and manufacturing of the bar; however, it results in a novel modular rotating boring tool.

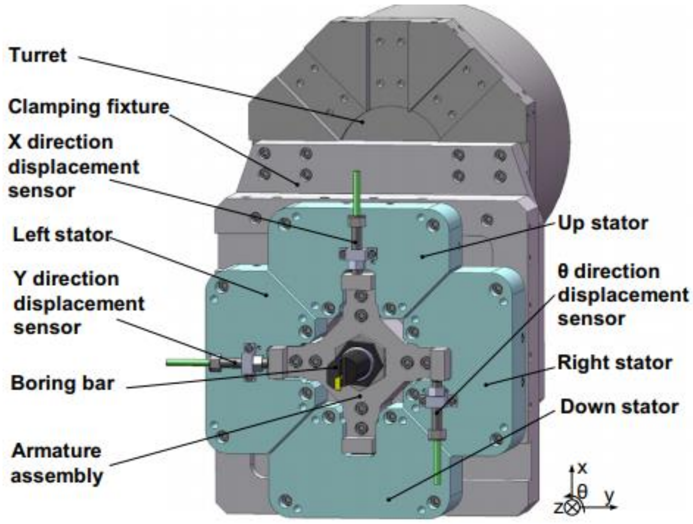

Figure 2.8: Electromagnetic actuator for active damping of boring bar chatter (Chen et al., 2014)

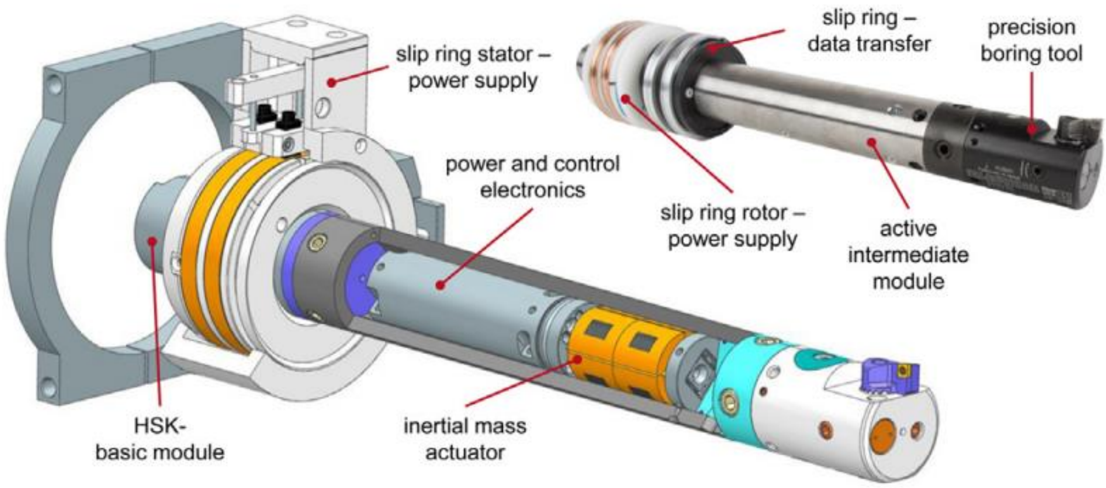

Figure 2.9: Electromagnetic inertial mass damper (Abele et al., 2016).

2.5 Magnetorheological fluid dampers

Magnetorheological fluids (MRFs) typically consist of ferrous micro and nano particles that are suspended in a carrier fluid with aid of some surfactants. These fluids undergo through fast and reversible phase change between liquid and solid states upon applying magnetic field. This change in properties, which is controlled by adjusting the magnetic field strength, gives the MRFs a potential to be utilized in several mechanical applications such as: brakes, clutches, and dampers (Carlson and Jolly, 2000).

In machining field, MRFs have been getting more attention in the last decade due to its controllable physical properties. It was reported in three main directions: MR polishing, MR flexible fixtures, and MR dampers for different machining operations as presented in Figure 2.10 (Lu et al., 2021). MRF is used for polishing of free-form geometries as shown in Figure 2.11 (Sidpara and Jain, 2013). Another application of MR fluids in machining field was presented by Kong et al., (2014) for chatter suppression in deep hole drilling. Their design allowed adjustments of the applied force location in addition to varying its magnitude by controlling the magnetic field. Recently, Liu et al., (2020) developed a controllable flexible fixture for machining of light structures such as thin-walled parts using MR fluids as shown in Figure 2.12.

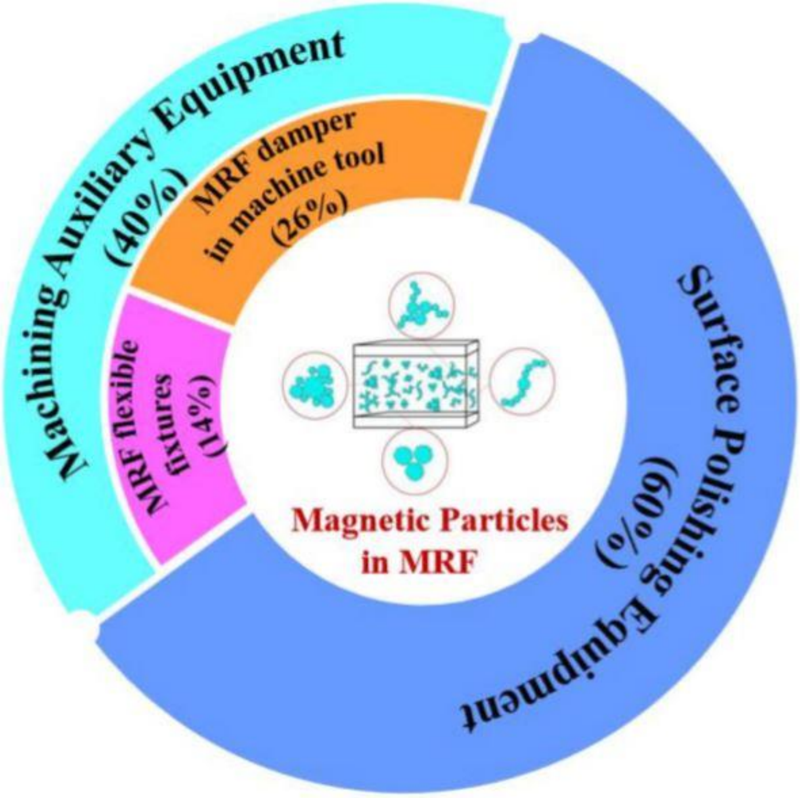

Figure 2.10: Classification of MRF usage in precision machining literature from 2016 to 2020 (Lu et al., 2021)

Figure 2.11: Polishing of free-form surfaces with MR fluid brush (Sidpara and Jain, 2013).

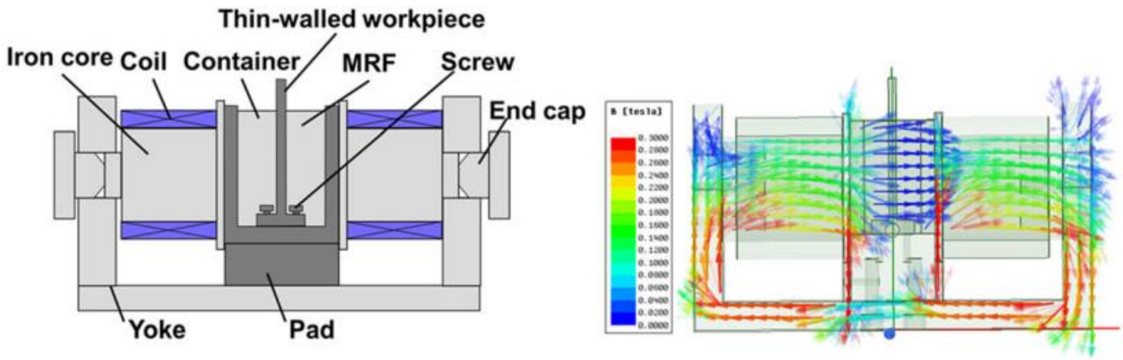

Figure 2.12: MRF flexible fixture for machining of thin-walled structures (Liu et al., 2020).

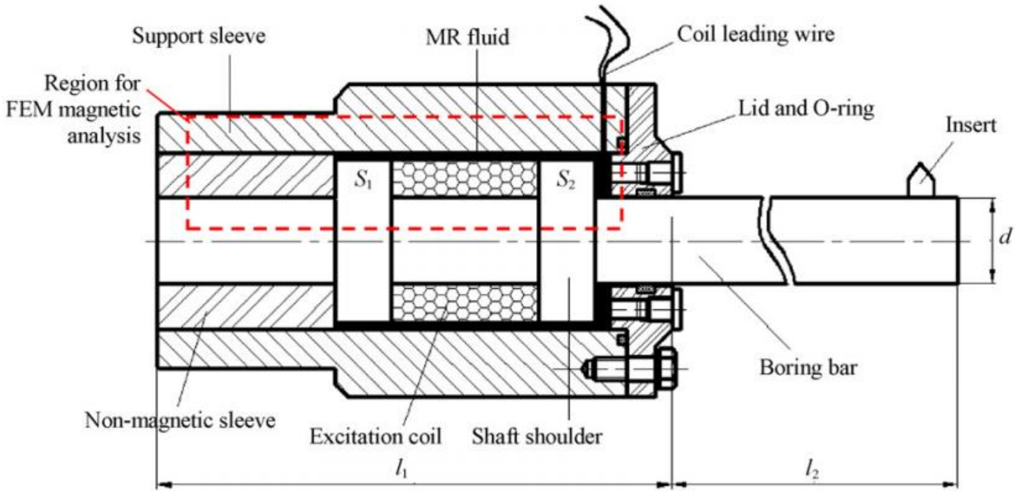

Figure 2.13: Schematic of the first MR fluid-controlled boring bar (Mei et al., 2009).

For the boring process, the first boring bar that utilizes MR fluid to control its stiffness was introduced by Mei et al. (2009). In their design as shown in Figure 2.13, the magnetic circuit is integrated with the boring bar as a single unit which increased the length of the boring bar which reduces its initial stiffness before activating the coil. In their analysis, they considered the effect of MR fluid only on the stiffness of the bar; however, both damping and stiffness are affected by activating the MR fluid. Moreover, their design requires a larger amount of the MR fluid and tight seals, which add more cost and complexity to the system compared to the design proposed in the present work. The system was experimentally tested on the boring setup shown in Figure 2.14. In their extended work, they used the same system for active damping of boring bar chatter by integrating it with an online chatter detection technique based on neural networks (Yao et al., 2010).

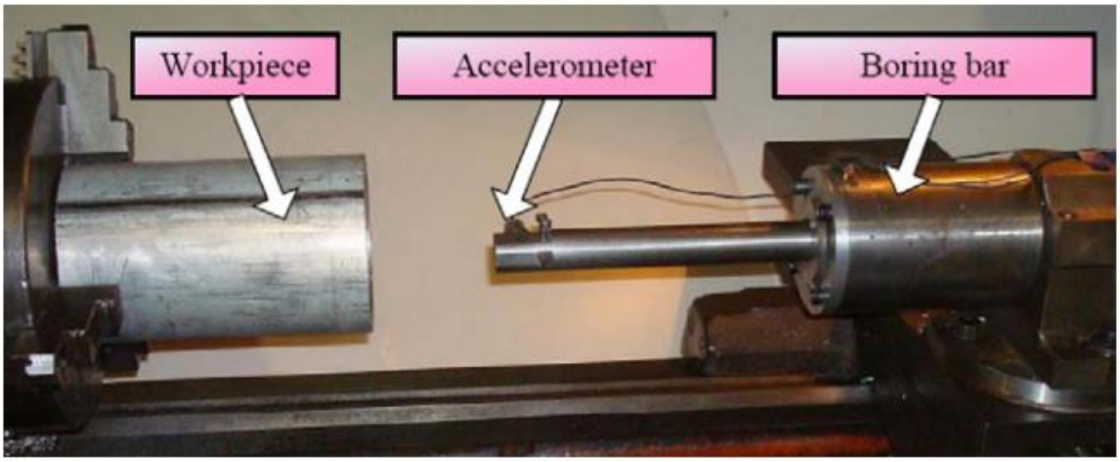

Figure 2.14: Experimental setup for active control of magnetorheological fluid boring bar (Yao et al., 2010).

Their design was inspired by a previously published work of Wang and Fei, (2001) who developed a tunable stiffness boring bar. In this design, they utilized electrorheological (ER) fluid as working substance to control the stiffness of the bar. ER fluids have controllable rheological properties like MR fluids, but they are actuated by varying the electric field. ER fluids require higher power consumption, and have a narrow temperature range, and less chemical stability compared to MR fluids.

Similar design of MR boring bar was used by (Kumar et al., 2017). The magnetic circuit is designed in finite element software. The main objective of their work is to investigate the effects of two synthesized MR fluids at different particle ratios on the roughness of machined surfaces. Two MR fluids with magnetizable particles at ratios of 40% and 36 % by volume were synthesized. The first one had high sedimentation rate within period of less than 5 days, while the other one had some additives to improve stability. They showed the improvement by visual inspection of the fluid samples without mention the numbers and the time frame. They performed many cutting experiments to find the optimum current for best surface roughness. However, this kind of experimental optimization is limited to the reported experimental work conditions and cannot be generalized.

Biju and Shunmugam (2018) introduced a special design of a boring bar with vibration transfer rod inside an MR fluid filled cavity as shown on the schematic diagram in Figure 2.15. They used the front part of a commercial boring bar at the tip side to keep the insert angles unchanged. Using a bar with different segments and an additional internal rod adds complexity to the design and implementation. They have shown that MR fluid can improve both the stiffness and damping of the boring process.

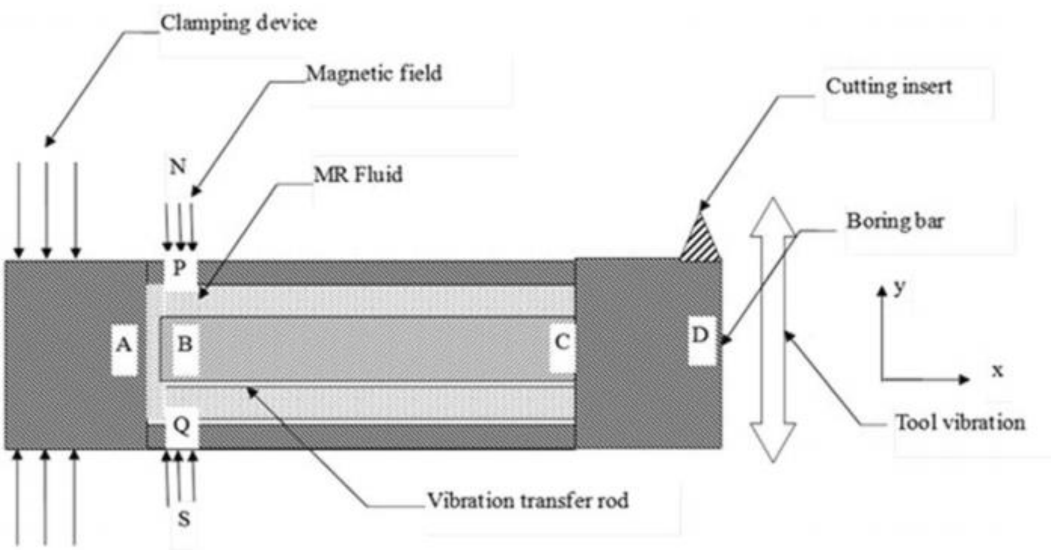

Figure 2.15: Schematic of magnetorheological fluid boring bar with transfer rod (Biju and Shunmugam, 2018).

Som et al., (2015) introduced an externally applied magnetorheological damper for baring bars. This external configuration, as shown in Figure 2.16, makes it easier in installation and allows for using commercial boring bars at different lengths. They showed that controlled damping can enhance stability of the boring process by increasing the chatter-free depth of cut on stability lobe diagrams. They applied the damping force in the tangential direction only which of course enhance stability during cutting process; however, in the boring process, the radial direction is much important when regenerative chatter is concerned. In this thesis, externally applied MR damper that provides damping effect in both radial and tangential cutting directions is proposed.

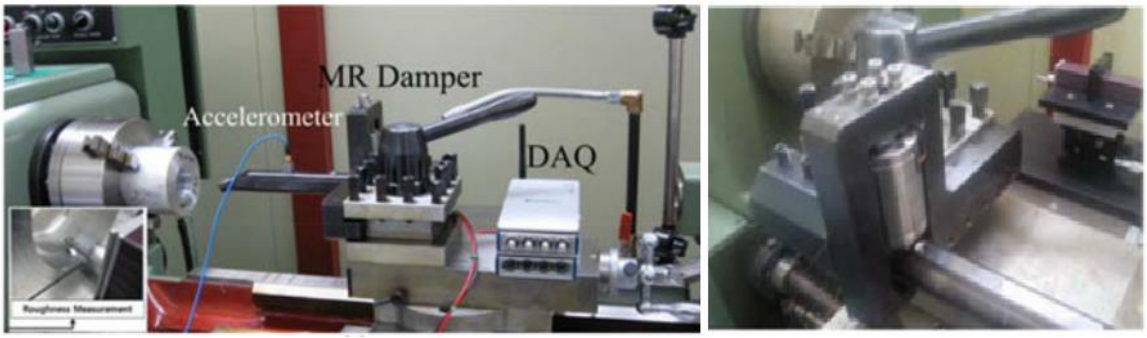

Figure 2.16: Externally applied MR damper for boring bars (Cao et al., 2017)(Som et al., 2015)

2.6 Control of magnetorheological fluid dampers

Control of magnetorheological dampers is important to make use of its unique properties such as fast response and controllable phase change that provides adjustable damping. Similar to electromagnetic actuators, power electronic amplifying circuits are needed to derive the required controlled electric current from DC power supply. Figure 2.17 describes the control flowchart of electromagnetic actuator for milling process (Wan et al., 2020).

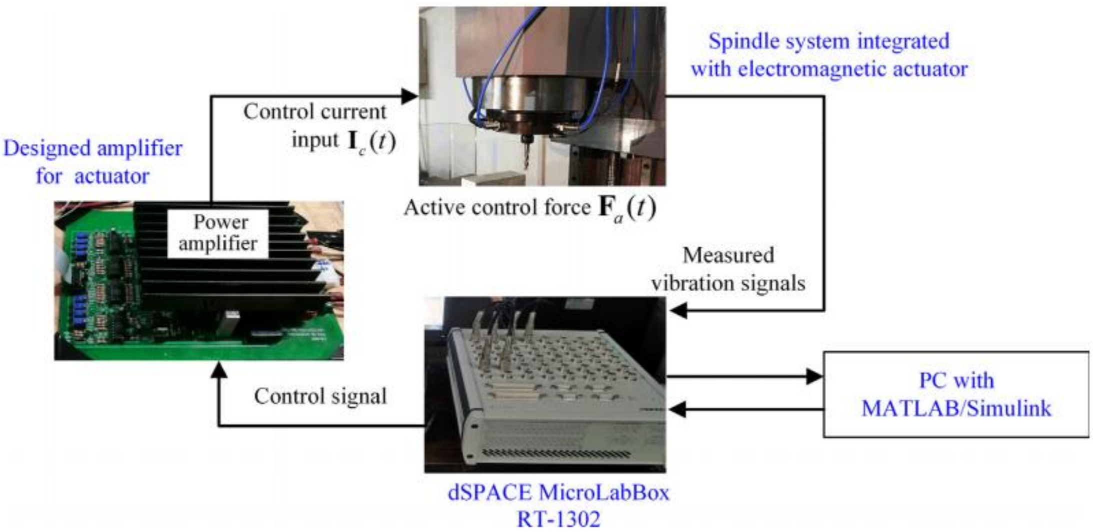

Figure 2.17: Experimental setup for active control of electromagnetic actuator for milling process.

In addition to the value of supplied electric current, the shape of its signal affects the generated damping forces. Mei et al., (2010) studied the effect of shape and frequency of the exciting current waveform on time-varying stiffness of magnetorheological fluid controlled boring bar. They found that square wave has better performance than triangular and sinusoidal waves. They used square wave current signal with amplitude of 2 A at low frequency range of 4-6 Hz. They studied the effect of varying the amplitude of the electric current on the natural frequency through experimental modal tap testing. Frequency varied between 123.7 and 157.2 Hz for current amplitude range of 0 to 2.5 A. Despite this controllable effect over natural frequency which is desirable, using very low frequency less than 10 Hz for the exciting current to control the boring bar at frequency above 120 Hz is questionable as some phase shift is expected. Moreover, they did not mention any details about the controller algorithm in their work.

In this thesis, square wave signals are generated in terms of pulse width modulated (PWM) signal. It is used to transmit the control command to the MR damper. As the MR damping forces depend on the magnetic field that is generated by the electromagnetic coil, the supplied current to the coil is adjusted by varying the duty cycle of the PWM signal. Moreover, sliding mode control algorithm is designed to control the MR damper.

2.7 Sliding mode control

Sliding mode control (SMC) is a robust control strategy that does not require accurate model of the plant. It can effectively compensate for unmodelled dynamics and parameter uncertainties. SMC has been reported in several machining applications.

Wan et al., (2020) introduced an active chatter suppression for the milling operation with sliding mode control. They developed an SMC model for the milling process with an electromagnetic actuator. In their work, they mentioned that static cutting forces can be neglected. Moreover, the time delay term of regenerative chatter is considered as disturbance to the system. Their simulations showed significant increase in chatter-free axial depth of cut in wide range of spindle speeds. Experimental validation cutting tests at different axial depth of cut were presented emphasizing the robustness of SMC and its potential for active damping of chatter in milling.

Moradi et al., (2009) studied chatter suppression in orthogonal turning using piezo actuator. The orthogonal turning is modelled as single degree of freedom system. Uncertainties in cutting velocity, tool wear, and dynamic model parameters were considered. They developed and compared two different control algorithms: H_∞ optimal control and sliding model control. Both controllers showed robustness against uncertainties; however, optimal control had smooth cutting force with less oscillations in time response, while SMC was able to achieve a faster response with less control effort.

Ma et al., (2020) proposed an adaptive sliding mode controller for chatter in turning operations. In their model, disturbances and parameter uncertainties are estimated using adaptive laws. The controller parameters are selected considering Lyapunov stability criteria. The controller is applied to the CNC turning machine through fast tool servo with piezoelectric element. Moreover, they used saturation functions to limit the control input to provide practical values depending on the actuator limitations.

In the boring process, Moradian et al., (2019) introduced an adaptive sliding mode controller for a piezo actuator. They considered the first three modes of operation in their derived model; however, they proved that considering first two, or three modes does not have much difference when compared to the first mode. Their simulations showed that adaptive SMC can improve the stability of the boring system in terms of displacement of the tip of the bar. Despite these optimistic simulation results, they did not provide any experimental validations.

The classical form of SMC has an inherent problem of chatter due to the discontinuous term in the control law. One solution to eliminate chatter is replacing the discontinuous term with a saturation function, but this approach reduces the robustness of the controller. Another solution is applying a second order sliding mode control which transfers the chattering effect to the higher derivatives keeping the control action chatter-free. An efficient approach to eliminate chatter of SMC is using the variable gain super twisting algorithm (VGSTA) (Gonzalez et al., 2012) or adaptive gain super twisting SMC (Shtessel et al., 2012). These approaches take the advantage of the continuous control of super twisting SMC, in addition to dynamically adjustment of the controller gains according to the actual bounds of the perturbations.

In this thesis, a second order sliding mode control with variable gain super-twisting algorithm is utilized to control the chatter of a boring bar integrated with the developed magnetorheological (MR) fluid damper for active chatter suppression in boring operation.

2.8 Research directions

As illustrated in the studied literature, magnetorheological fluids have a great potential in damping of mechanical vibrations. The controllable rheological properties can offer adjustable stiffness and damping to the boring bar and enhance the stability of the process. MR damper based on sponge-type configuration is proposed to reduce the required MR fluid and eliminate sealing requirements. This design offers a cost-effective solution for chatter problem. The damper is designed to be easily installed on CNC turning centers and to be utilized with commercial boring bars to be applicable in industry.

Active control system is designed to benefit from the controllability of the MR fluid properties and offer better damping for wide range of operating conditions. Active damping system based on sliding mode control (SMC) is presented in this thesis. SMC with variable gain super twisting algorithm is derived for the boring process to eliminate the chatter problem of classical SMC and ensure its robustness against disturbances and parameter uncertainties.

The effectiveness of the proposed system is shown on stability lobe diagrams and experimentally verified on boring tests of Al7075 and Inconel 718 workpieces under various cutting conditions.

Chapter 3

DESIGN OF MAGNETORHEOLOGICAL DAMPER FOR BORING BARS

3.1 Overview

Magnetorheological fluids, with their unique property of fast and reversible phase change between solid and liquid states, can provide a controllable damping effect for several dynamic applications. In this chapter, a novel solution for damping chatter vibrations in the boring process, based on sponge-type magnetorheological fluid technology, is introduced. The damper is designed to be installed on CNC turning center and to be utilized for different commercial boring bars. A new bidisperse MR fluid with competitive characteristics that was developed by the chemistry lab at Koç university, is utilized in this damper. The electromagnetic circuit is designed and analyzed in FEM environment and parametric analysis were performed to obtain the final dimensions. The proposed damping system provides an efficient solution for one of current problems in machining industry.

3.2 Design considerations

The design of magnetorheological damper for boring bars is presented in this chapter. The sponge type configuration is selected as it reduces the required amount of the MR fluid which is the most expensive part of the MR devices. Moreover, this configuration does not need tight sealing to keep the MR fluid in the desired space which results in simpler design with low cost (Chrzan and Carlson, 2001).

The proposed MR damper is designed to be installed on CNC turning center as shown on the CAD model in Figure 3.1. It is designed in cylindrical shape to provide damping in both radial and tangential cutting directions of the boring bar. It can be used for both right-hand and left-hand boring bars. To provide practical solution, the proposed damper allows easy installation, adjustable length of the bar, and using of different commercials boring bars.

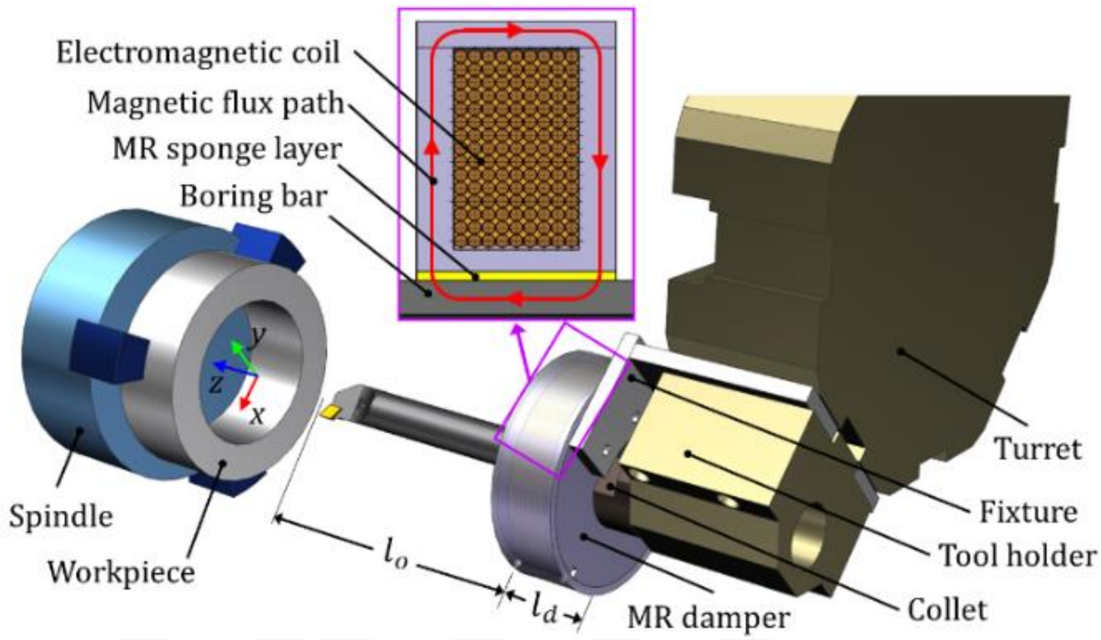

Figure 3.1: CAD model of the boring bar with the MR damper on the turning center. Inset: cross-sectional view of the MR damper.

The components of the MR damper are presented in the exploded view of the CAD model as given in Figure 3.2. It is showing that the damper consists of three main components: MR sponge layer, electromagnetic circuit assembly, and damper fixture.

The electromagnetic coil is required to provide the exciting magnetic flux to the MR fluid in the sponge layer. The assembly consists of an electromagnetic coil made of thin copper wire, a bobbin composed of an inner cylinder and two side flanges forming a U-shape cross-sectional area to wrap the coil inside it, and an outer cylinder to provide the retaining path of the electromagnetic flux. Both the bobbin and outer cylinder are made from low carbon steel grade AISI 1020 because of its good magnetic permeability. The bobbin is manufactured as a single piece to avoid leakage of magnetic flux, while the outer cylinder is separately manufactured and assembled to it with tight fit after wrapping the coil wire. A standard copper wire of gauge AWG 28 is selected to ensure high magnetic flux with rated current of 0.25 A.

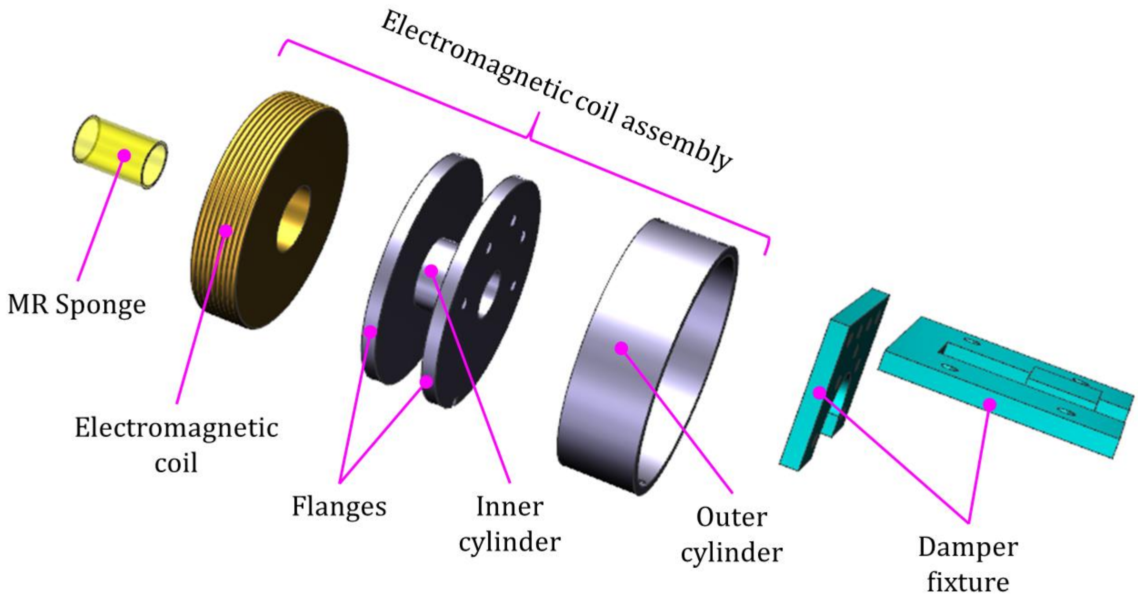

Figure 3.2: CAD model of MR damper components in exploded view

The damper is attached to the tool holder and the turret of the CNC machine by a fixture, made from a non-magnetic material to avoid flux leakage. This fixture is manufactured from two Aluminum pieces to provide easy installation procedure. It is attached to the damper by four stud bolts to confirm the axial alignment of the damper with the boring bar, and to make their installation to the conventional tool holder of the CNC machine tool straightforward.

For the sponge layer, a polyurethane foam sheet of 2 mm thickness is wrapped around the bar and serves as fluid retainer to contain the MR fluid inside the cylindrical gap between the boring bar and the electromagnetic coil. The average pore size of the utilized foam is about 500 microns. Figure 3.3 shows the scanning electron microscope SEM image of the used foam layer before being filled with the MR fluid. As this configuration minimizes the required MR fluid amount, only 15 ml of bidisperse MR fluid is used in the damper.

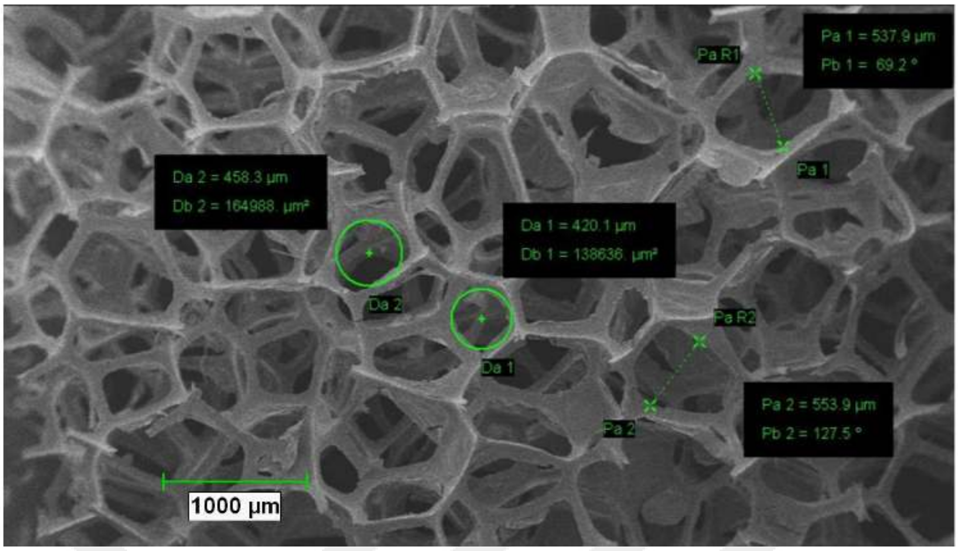

Figure 3.3: SEM image of the polyurethane foam layer

3.3 Bidisperse MR fluid

Magnetorheological fluid is the basic element of the proposed damper. Typical magnetorheological fluids MRFs are composed of micron-sized magnetizable particles suspended in a hydrocarbon carrier fluid. These particles quickly respond to the external magnetic field forming a chain-like structure that increases the viscosity and yield stress of the fluid. Particle loading influences the magnetorheological properties and is usually kept around 80 wt% in commercial MRFs. One major problem of these MRFs is quick sedimentation of the dense large particles, forming hard to re-disperse agglomerates, which limits the lifetime of MR devices. Since a small amount of a stable MRF with good magnetorheological properties is desired to be implemented to the proposed damper, a custom bidisperse MRF, composed of micro and nano-sized magnetizable particles, is synthesized in the chemistry lab at Koç university. In bidisperse MRFs, some of the dense micron-sized particles are replaced with magnetic or nonmagnetic nanoparticles. These nanoparticles prefer thermodynamic colloidal dispersions over sedimentation under gravity which leads to slower sedimentation of the large particles (Ngatu and Wereley, 2007). Under magnetic field, while micron-sized CI-LA forms chain-like structure by aligning with the external field, nanoparticles are supposed to fill in the gaps to provide better chaining and alignment to enhance magnetorheological properties while reducing sedimentation at rest, which is a serious problem of MRFs.

For the fabrication of the bidisperse MRF, Poly(acrylic)acid coated superparamagnetic iron oxide nanoparticles (SPION-PAA) (5-10 nm) are synthesized and utilized as magnetic nanoparticles. The transmission electron microscopic (TEM) image of the synthesized SPION-PAA is shown in Figure 3.4 (a). Commercial carbonyl iron particles (Sigma Aldrich, 2-5μm) are used as micron-sized particles after being coated with lauric acid (CI-LA) to reduce particle aggregation and improve its stability in the carrier fluid. Bidisperse MRF is prepared by 71 wt% CI-LA, 12 wt% in SPION-PAA, and 3 wt% polyvinyl alcohol (PVA) in hydraulic oil (Mobil DTE 27) using a light-duty homogenizer at 12000 rpm. Figure 3.4 (b) shows the yield strength of the developed bidisperse MRF versus the magnetic field intensity. The inset in this figure illustrates that this bidisperse MRF even at such high particle loading (compared to commercial Lord 132DG or 140CG) stayed stable without sedimentation for more than four months which is not possible with commercial MRFs.

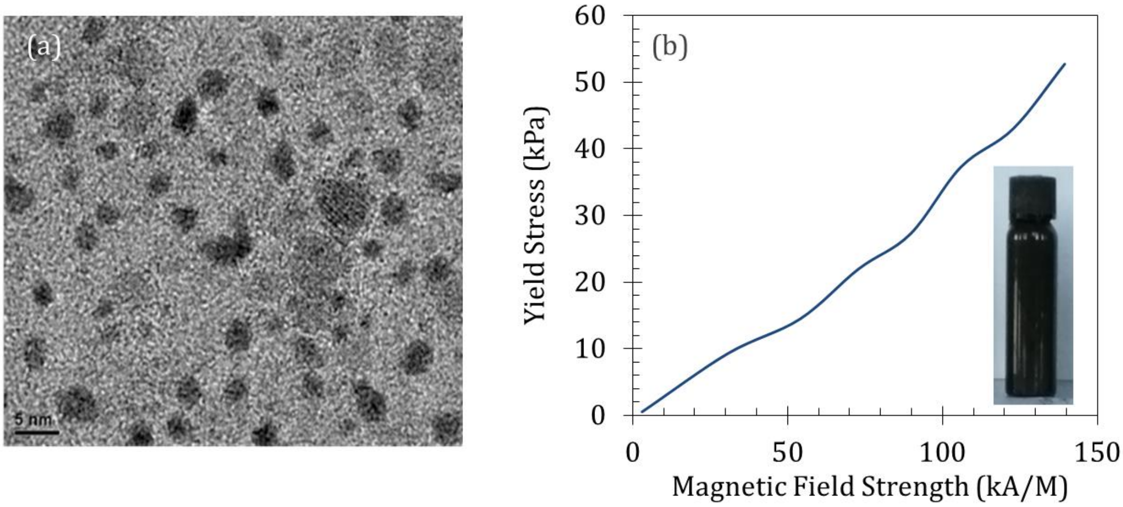

Figure 3.4: (a) TEM image of the synthesized SPION-PAA. (b) Yield stress versus magnetic field strength. Inset: Stability of bidisperse MRF after 4 months (no sedimentation)

3.4 Electromagnetic circuit design

3.4.1 Overview

Design of the electromagnetic circuit is crucial for MR devices to ensure sufficient magnetic flux in the effective zone to activate the MR fluid. As stated before, materials with high permeability should be selected for the parts where the magnetic flux passes; however, most of these materials have nonlinear magnetic properties as it naturally saturates after certain limit of flux intensity as shown in the B-H curve of the chosen material AISI 1020 in Figure 3.5. To consider this phenomenon and to obtain realistic results, finite element analysis FEA of the magnetic circuit were performed on COMSOL Multiphysics software where B-H curves of the used materials are included to get much accurate results. Moreover, values of different geometric parameters were varied in specific range to get the minimal dimensions of the damper for the highest magnetic flux.

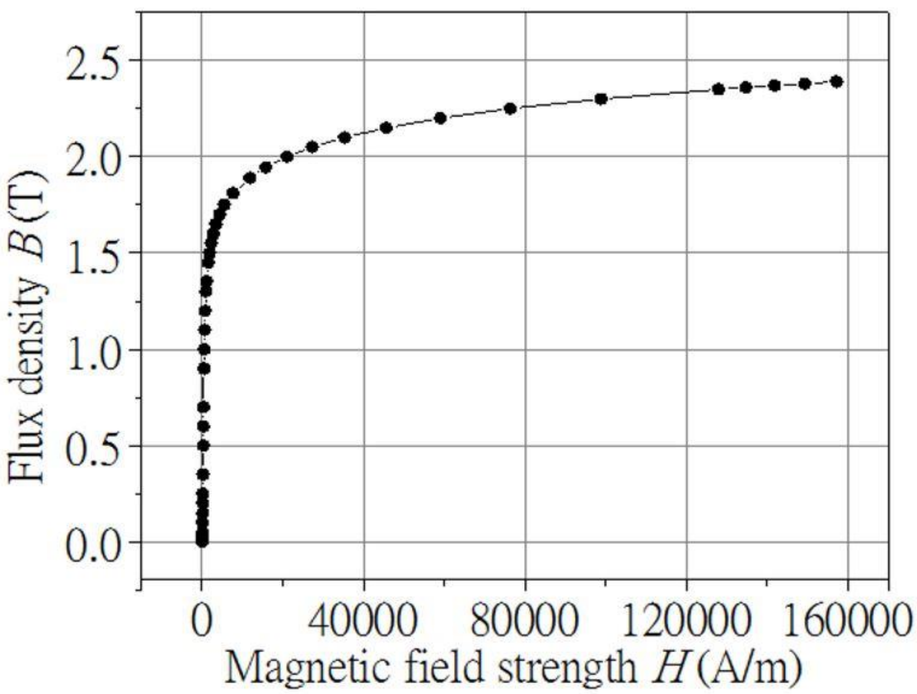

Figure 3.5: B-H curve of AISI 1020 steel (Tran and Hwang, 2020).

3.4.2 Finite element model of the electromagnetic circuit

The electromagnetic circuit is analyzed in FEM environment to have realistic values regarding saturation and distribution of the magnetic flux in different sections of the damper. The geometry is built as 2D axis symmetric model and analyzed using the submodule of magnetic fields under the AC/DC module in COMSOL Multiphysics software. The cross-sectional area of the damper is shown in Figure 3.6. The materials are assigned to each part from the built-in library of the software to utilize their predefined magnetic properties and B-H curves. The inner cylinder, outer cylinder and the flanges are assigned as steel AISI 1020, the electromagnetic coil is defined as copper coil with specified wire gauge, the boring bar made from carbide steel, and the damper fixture is made from Aluminum.

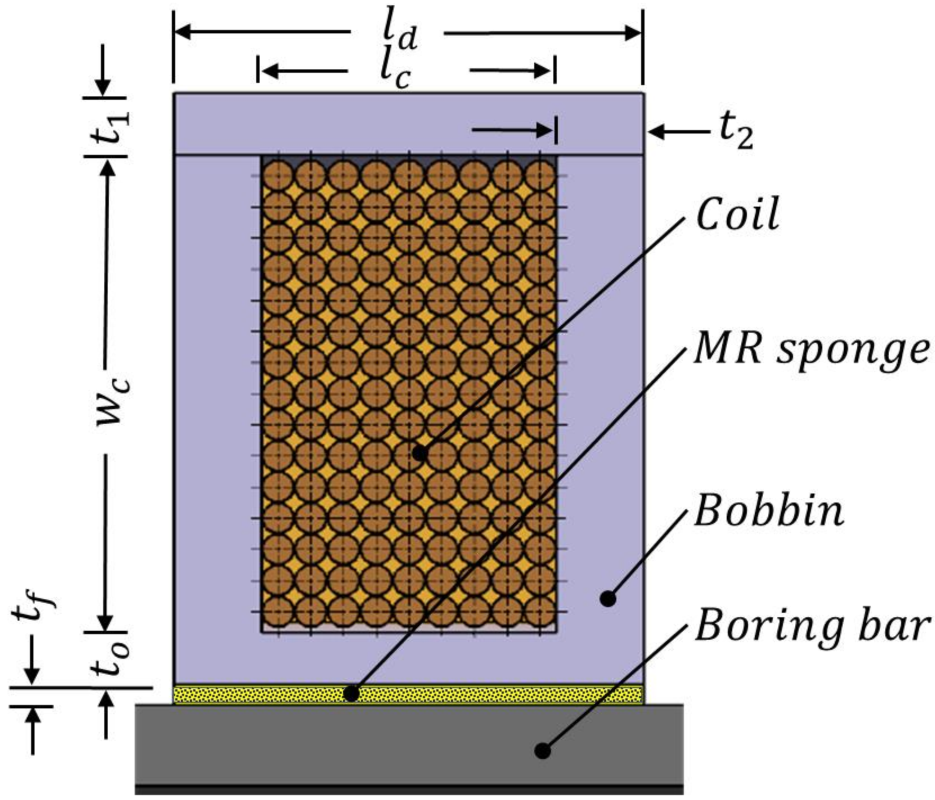

Figure 3.6: Dimensional parameters on 2D cross-sectional view of the MR damper.

The magnetic flux distribution is shown on the 2D cross-sectional view in Figure 3.7. The equivalent 3D model results are shown in Figure 3.8. Average magnetic flux of 1 T is targeted on the edge of the boring bar in the effective region of the MR sponge layer which is sufficient to excite the MR fluid to obtain the desired yield stress.

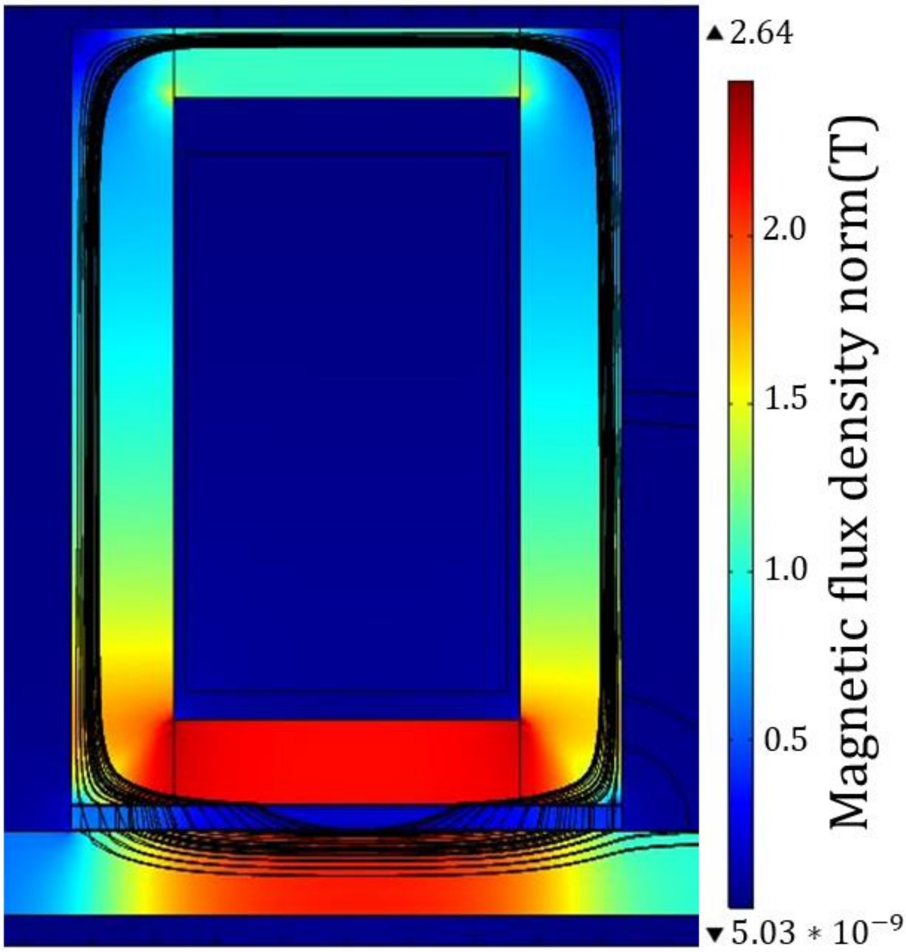

Figure 3.7: FEM results of magnetic flux with flux lines in the sponge zone.

3.4.3 Parametric analysis of the electromagnetic circuit

Many geometric parameters influence the results of the magnetic flux intensity in the desired zone. Parametric sweep technique is used to optimize the geometry of the new MR damper. Each variable value is swept through a specific range with respect to other variables. Some limitations due to space availability or manufacturing capabilities are considered. The main limiting factor through this process is the magnetic flux saturation in different segments of the electromagnetic circuit components.

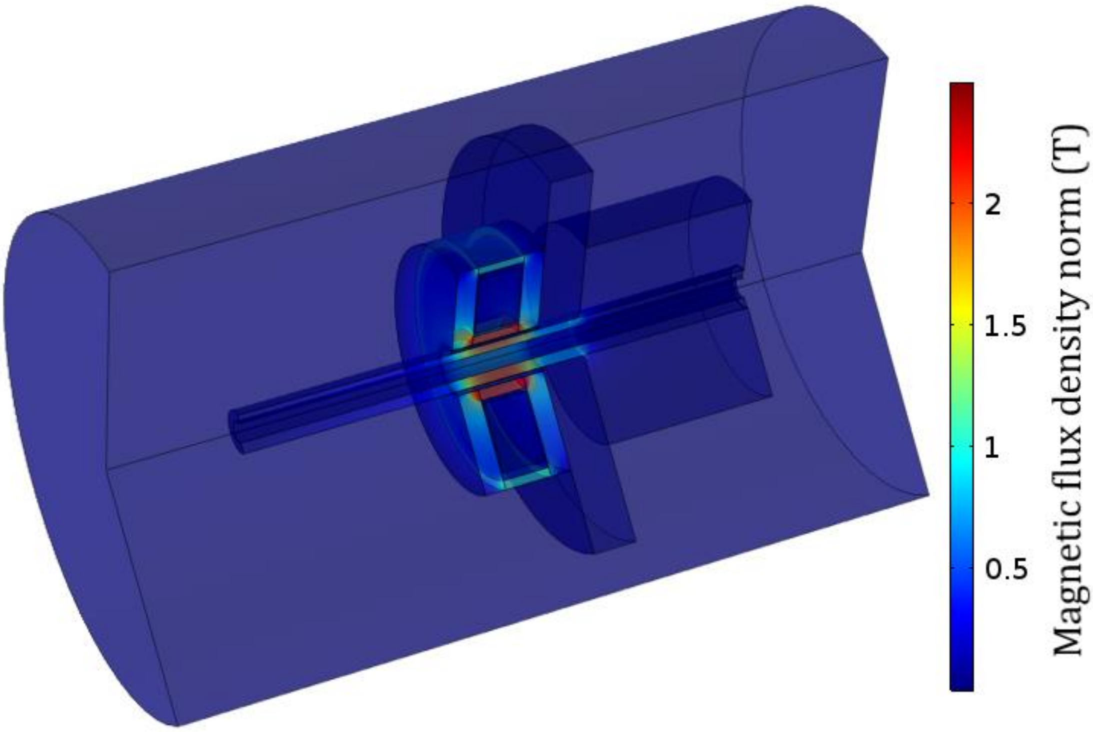

Figure 3.8: Equivalent 3D FEM results of magnetic circuit design.

Dimensional parameters of the proposed design are given in Figure 3.6. l_c and w_c are length and width of the electromagnetic coil, respectively. The value of l_c is selected so that maximum length of the damper l_o does not exceed 15% of the total bar length in order to keep the ratio of the overhang length to the diameter of the boring bar greater than six. The value of w_c is defined based on the number of turns (N) of the coil. number of turns N value is swept from 1000 to 7000 turns as shown in Figure 3.9. Although increasing the number of turns leads to higher magnetic flux in the effective zone, the rate of increase after 4000 turns is relatively low as shown in Figure 3.10. However, the number of turns of the electromagnetic coil is decided to be 5000 turns to compensate for the loss of magnetic flux due to manual wrapping of the coil.

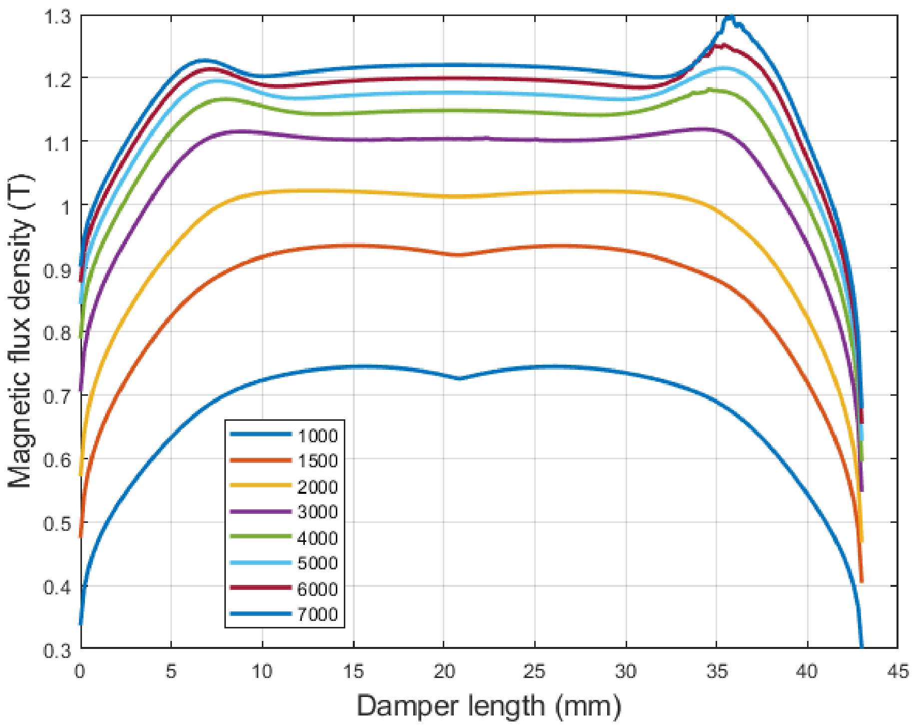

Figure 3.9: Magnetic flux density on the sponge layer at different values of number of turns

The other geometric parameters that affect the magnetic flux intensity in the effective zone of MR sponge layer, are the thickness of different portions the magnetic flux path such as, the inner and outer cylinders and the side flanges of the damper.

Thickness of the outer cylinder t_1 is varied from 1 to 7 mm. The variation of magnetic flux density along the damper length in the effective zone due to outer cylinder thickness variation is given in Figure 3.11. Increasing the thickness t_1 increases the magnetic flux up to a saturation value of 1.01 T at 4 mm thickness as shown in Figure 3.12.

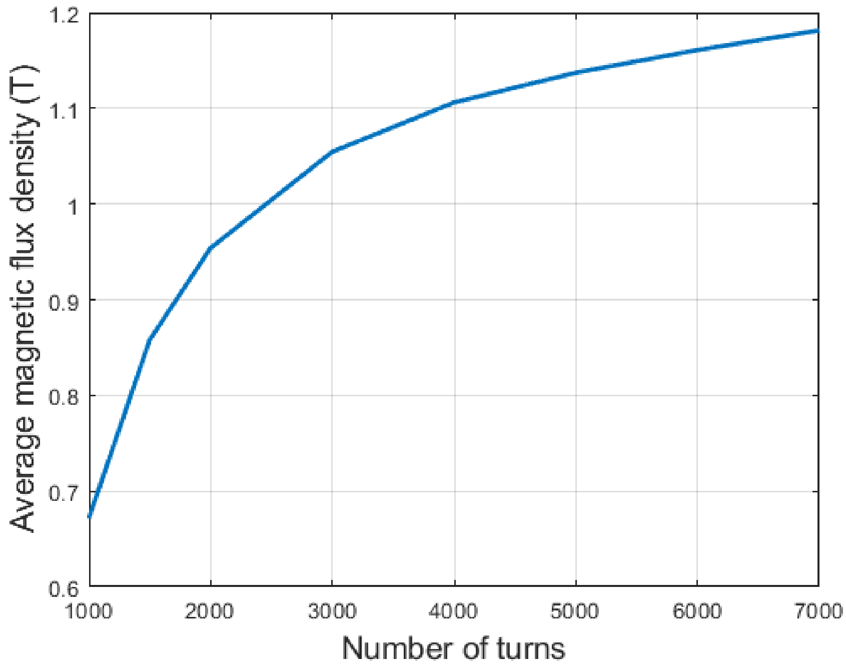

Figure 3.10: Effect of number of turns of the coil on the average magnetic flux.

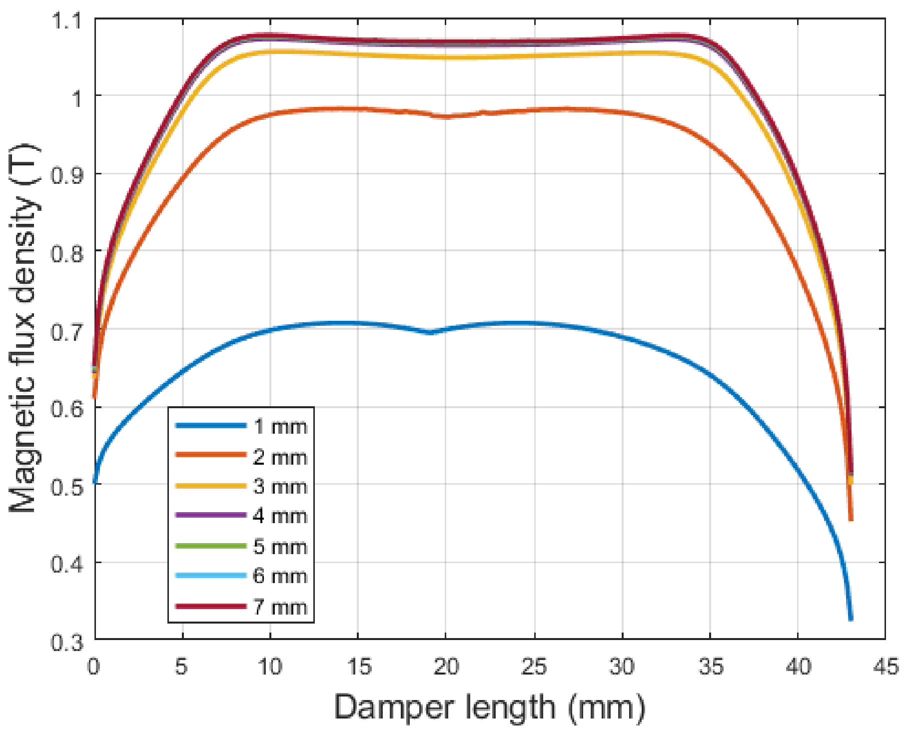

Figure 3.11: Magnetic flux density on the sponge layer at different values of outer cylinder thickness.

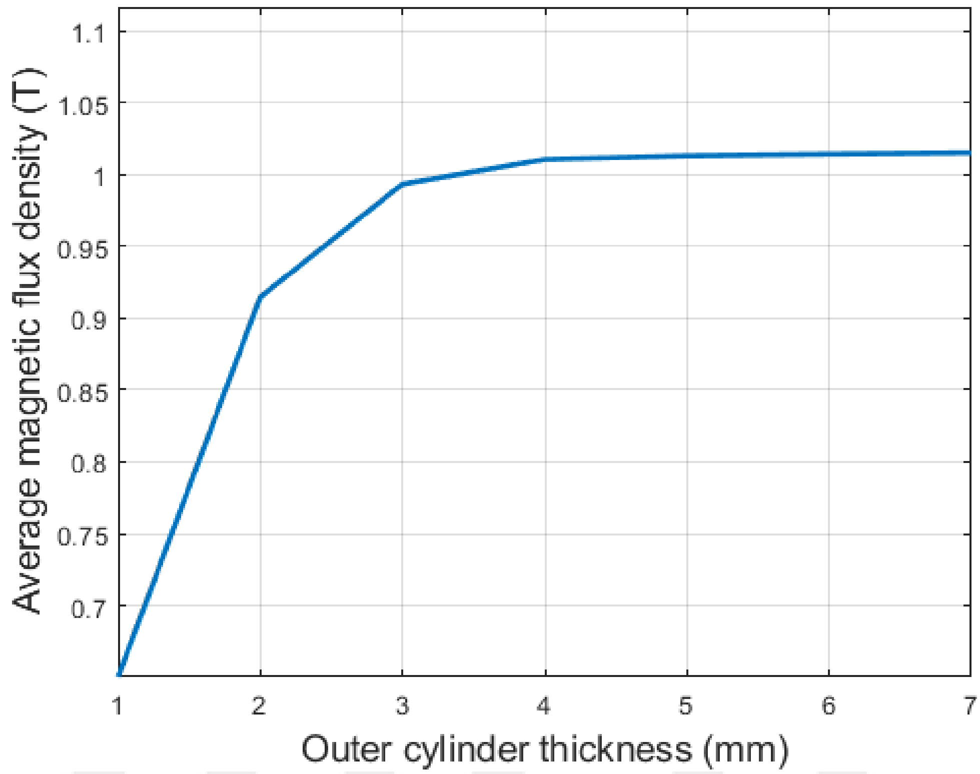

Figure 3.12: Effect of outer cylinder thickness variation on the magnetic flux.

The effect of the side wall thickness on the average magnetic flux in the target zone is presented in Figure 3.13. It shows a peak value at 8 mm thickness. For the inner cylinder, increasing the thickness leads to less magnetic flux density in the sponge layer as most of the flux passes through the thicker part of the inner cylinder because of its higher permeability. Figures 3.14 shows the effect of inner cylinder thickness variation on the magnetic flux density in the sponge zone. Smaller the thickness, higher magnetic flux is obtained as shown in Figure 3.15; however, the value of 6 mm is selected for manufacturing constraints as the flux decreases with higher slope after this value.

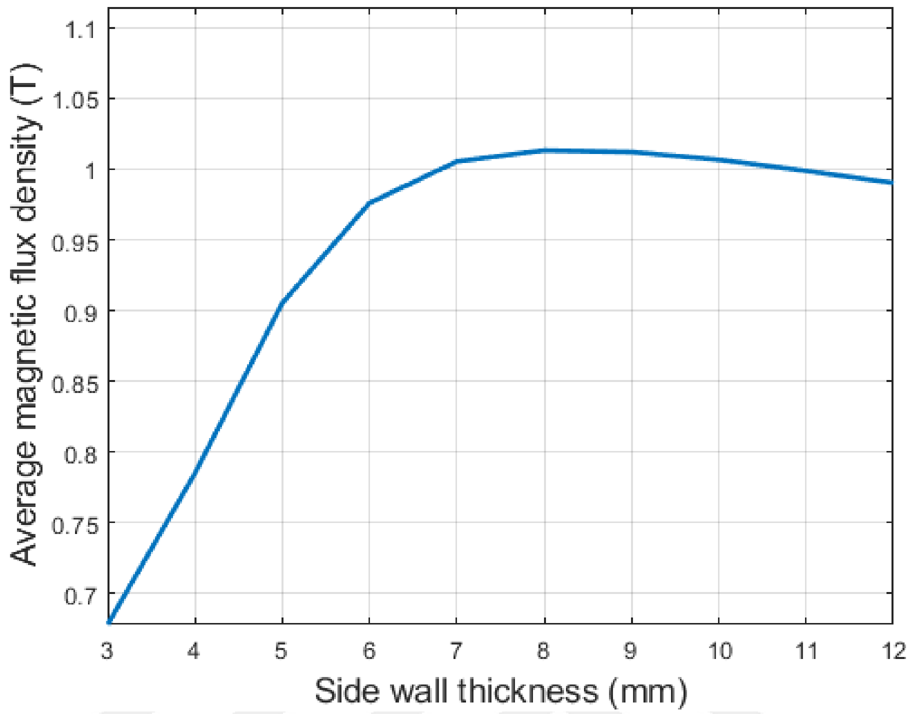

Figure 3.13: Effect of side wall thickness variation on the magnetic flux density

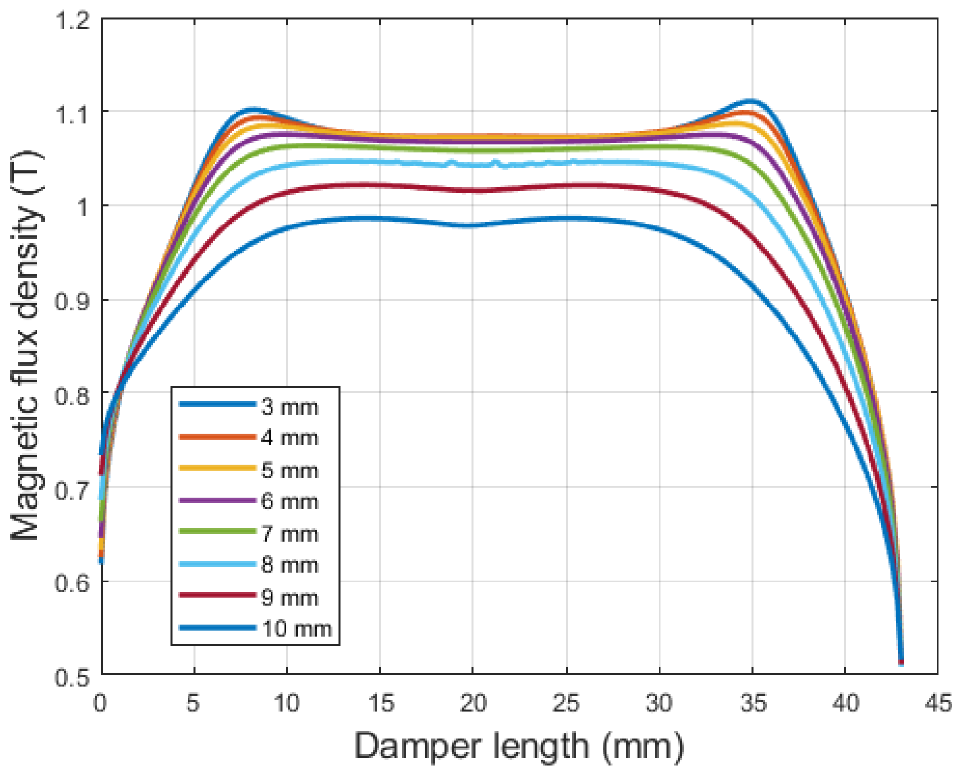

Figure 3.14: Magnetic flux density on the sponge layer at different values of inner cylinder thickness.

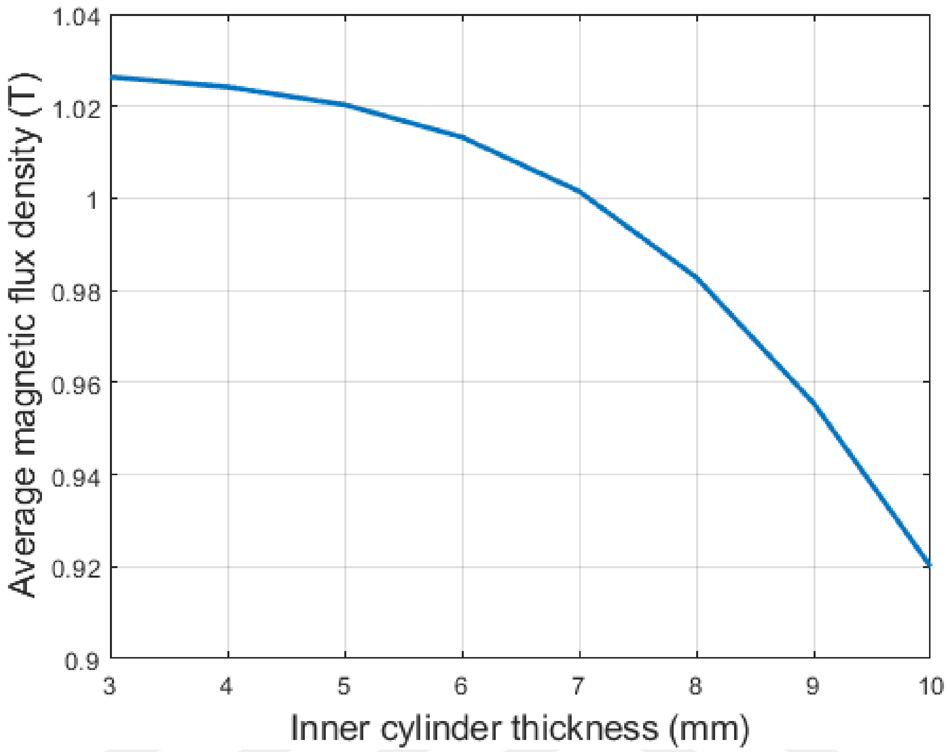

Figure 3.15: Effect of inner cylinder thickness variation on the magnetic flux.

3.4.4 Final design of the electromagnetic circuit

The design of the damper is completed based on the FE analysis and the parametric sweep results and considering manufacturing and installation limitations. The final dimensions of the damper are given in Table 3.1.

Table 3.1: Dimensions of the MR damper

Parameter		Value (mm)
Coil length	l_c	27
Coil width	w_c	45
Damper length	l_d	43
Inner cylinder thickness	t_o	6
Outer cylinder thickness	t_1	4
Side wall thickness	t_2	8
MR layer thickness	t_f	2

Chapter 4

CONTROLLER DESIGN

4.1 Overview

The designed MR damper, with its controllable rheological properties and fast response, is considered as promising alternative for active damping systems in machining operations. To achieve that, a robust control system is developed and implemented on the designed MR damper for boring bars. The sliding mode control (SMC) is selected for controller design due to its known robustness against disturbances and its tolerance to unmodelled dynamics and parameters uncertainties. These properties are proven in simulation results and experimental cutting tests. The controller showed good and fast response. Simulations of the proposed controller are compared with the widely used PID controller at wide frequency range.

4.2 System modeling

The boring bar and the magnetorheological (MR) damper are installed on the turret of a CNC turning center as shown in the CAD model in Figure 3.1. Due to the typical structure of the boring process, the boring bar is often modeled as a continuous cantilever beam with fixed end on the turret side and a free end on the insert tip; however, the first natural frequency dominates the performance of the bar as illustrated in several articles in literature (Moetakef-Imani and Yussefian, 2009) (Moradian et al., 2019). In this work and based on the modal analysis results which show a single dominating frequency in the lateral direction, the bar is simplified to a single degree spring-mass-damper system. Since the chatter in the boring process occurs in the radial direction, the lateral motion of the boring bar at the insert tip along x-axis is modeled as shown in Eq. (4-1).

$$m\ddot{x} + c\dot{x} + kx = F_c + u \tag{4-1}$$

where *m, c,* and k are the modal mass, damping, and stiffness of the system, F_c is the cutting force in the radial direction, and u is the control force which is provided by the magnetorheological damper. The cutting force during regenerative chatter in the radial direction is defined as in Eq. (4-2).

$$F_c = k_c w_c (h_o + d(t)) \tag{4-2}$$

The cutting force coefficient in the radial direction k_c is obtained using the well-known orthogonal to oblique transformations in the force calibration tests of the used workpiece material (Altintas, 2012). w_c and h_o are the width and nominal depth of cut respectively. The term $d(t)$ represents the dynamic chip thickness due to regenerative chatter in the spindle period of τ as explained in Eq. (4-3). The system in (4-1) is expressed in state-space form as in Eq. (4-4).

$$d(t) = x(t - \tau) - x(t) \tag{4-3}$$

$$\begin{bmatrix} \dot{x}_1 \\ \dot{x}_2 \end{bmatrix} = \begin{bmatrix} 0 & 1 \\ -\frac{k}{m} & -\frac{c}{m} \end{bmatrix} \begin{bmatrix} x_1 \\ x_2 \end{bmatrix} + \begin{bmatrix} 0 \\ \frac{1}{m} \end{bmatrix} F_s + \begin{bmatrix} 0 \\ \frac{k_c w_c}{m} \end{bmatrix} d(t) + \begin{bmatrix} 0 \\ \frac{1}{m} \end{bmatrix} u(t) \tag{4-4}$$

The static force $F_s = k_c w_c h_o$ will be ignored in the controller design as it does not contribute to the chatter, and the dynamic thickness $d(t)$ will be involved in the disturbance term.

4.3 Controller Design

4.3.1 Sliding mode control

Sliding mode control SMC has been recognized as robust control with high tracking accuracy and finite time convergence. In this work, as a simplified model of the system is considered and in the presence of disturbances such as chatter vibrations during the boring process, SMC is considered as potential controller strategy because it compensates for unmodelled dynamics with high robustness against disturbances.

The objective of the controller is to keep the displacement of the bar at the desired value $x_d = 0$ during the cutting process. To achieve this goal in the presence of dynamic disturbances, a robust sliding mode controller with variable gains is developed. Two new coordinates are introduced as $\sigma = \frac{1}{m}(x_1 - x_d)$ and $\rho = mx_2$, and the system can be written as in Eq. (4-5) and (4-6).

$$\dot{\sigma} = \frac{1}{m^2}\rho \tag{4-5}$$

$$\dot{\rho} = -cm\dot{\sigma} - km\sigma - kx_d + w(t) + u \tag{4-6}$$

where $w(t) = k_c w_c d(t)$ is the disturbance term. The sliding surface with a sliding coefficient K is defined as in Eq. (4-7).

$$s = \rho + K\sigma \tag{4-7}$$

When the system states reach the sliding surface $s = 0$, it results in a reduced-order system $\dot{\sigma} = \frac{K}{m^2}\sigma$. Writing the system in terms of σ and s as state variables with an equivalent control law of Eq. (4-8), the new system can be represented by Eq. (4-9) and (4-10).

$$u = -\frac{K}{m^2}(-K\sigma + s) + cm\dot{\sigma} + km\sigma + kx_d + v \tag{4-8}$$

$$\dot{\sigma} = \frac{1}{m^2}(-K\sigma + s) \tag{4-9}$$

$$\dot{s} = v + w \tag{4-10}$$

4.3.2 Sliding mode control with variable gain super-twisting algorithm

The conventional sliding mode control has good properties to reject disturbances and tolerate uncertainties in the system model, but at the same time it has an inherent problem of chatter due to the discontinuous term of the signum function. This phenomenon has been resolved by some techniques like sigmoid function or quasi sliding mode as mentioned in (Shtessel et al., 2014). This approach provides a smooth control action, but at the cost of deterioration of robustness. The proposed controller which utilizes the method of variable gain super-twisting algorithm VGSTA is unique as it offers the advantages of the classical sliding mode control along with a continuous control action (Gonzalez et al., 2012). Similar approaches named adaptive gain super twisting sliding mode controller are proposed by Shtessel et al., (2012) and Xiong et al., (2019). The proposed controller in this thesis is derived based on the model of (Gonzalez et al., 2012) as defined by Eq. (4-11).

$$v = -k_1(t,x)\emptyset_1(s) - \int_0^t k_2(t,x)\emptyset_2(s)dt \tag{4-11}$$

where,

$$\emptyset_1(s) = |s|^{\frac{1}{2}}\, sign(s) + k_3 s \ \ , k_3 > 0 \tag{4-12}$$

$$\emptyset_2(s) = \frac{\partial\emptyset_1(s)}{\partial s}\emptyset_1(s) = \frac{1}{2}sign(s) + \frac{3}{2}k_3|s|^{\frac{1}{2}}\, sign(s) + k_3^2\, s \tag{4-13}$$

The variable gains $k_1(t,x)$ and $k_2(t,x)$ make the sliding surface insensitive to the growing bounded perturbations, while the constant $k_3 > 0$ deals with the linearly growing perturbations out of the sliding surface.

As the perturbation w and its time derivative $\dot{w}$ are functions of the state variables and they take the form of summation of some harmonics, they are assumed to be bounded by a known harmonic function. The perturbations $w(t)$ can be further approximated as $w(t) = \tau\dot{x}$ (Moradian et al., 2019). The variable gains are given by Eq. (4-14) and Eq. (4-15).

$$k_1(t,x) = \delta + \frac{1}{\beta}(\frac{1}{4\epsilon}\mu^2(t,x) + 2\epsilon\mu(t,x) + \epsilon + 2\epsilon(\beta + 4\epsilon^2)) \tag{4-14}$$

$$k_2(t,x) = \beta + 4\epsilon^2 + 2\epsilon k_1(t,x) \tag{4-15}$$

where δ, β, and ϵ are arbitrary positive constants, and $\mu(t,x)$ is a known continuous function dependent on the state σ and the derivative of the perturbation bounds as given in Eq. (4-16).

$$\mu(t,x) \geq \frac{2k_c w_c}{m} K\dot{\sigma} \tag{4-16}$$

4.3.3 Control of the magnetorheological damper

The control input $u(t)$ is applied to the boring bar by activating the coil of the magnetorheological damper with a DC power source. As explained in the schematic diagram in Figure 3.1, the damper is attached next to the turret and tool holder, while chatter happens at the tip of the bar where the insert-workpiece interaction takes place. For this reason, the required force by the controller u is magnified using the lever rule to decide the actuation force F_a generated by the MR damper as in Eq. (4-17).

$$F_a = u\,(l_o + l_d)/(l_d\,/\,2) \tag{4-17}$$

where l_0 is the overhang length of the bar and l_d is the axial length of the MR damper. The acting force F_a is assumed to be concentrated at the middle of the length l_d. This force is a function of the surface area of the sponge layer A_{MR} and the MR yield stress τ_{MR}. The relation between yield stress and electric current is approximated by linear relationship with slope K_{MR} in the working range of the damper as shown in Figure 3.4 in the previous chapter. The electric current of the MR damper can be written as in Eq. (4-18).

$$i(t) = \frac{\tau_{MR}}{K_{MR}} = \frac{1}{K_{MR}}(F_a(t)/A_{MR}) \tag{4-18}$$

The supplied voltage to the damper is determined based on the values of the inductance L and the resistance R of the electromagnetic coil as in Eq. (4-19).

$$V(t) = R\,i(t) + L\frac{di}{dt} \tag{4-19}$$

4.4 Simulation results

The developed control algorithm is simulated in the Simulink environment as explained in Figure 4.1. The controller parameters are selected so that the Lyapunov stability is ensured, and its conditions are satisfied. However, according to (Shtessel et al., 2014) and (Shtessel et al., 2012), the gains are tuned through simulations until a satisfactory performance is achieved. The sliding coefficient K and the controller parameters δ, β, and ϵ are designed based on the Lyapunov stability criteria as explained in (Gonzalez et al., 2012). Their values for the designed controller are set as $K = 10$, $\delta = 0.1$, $\beta = 7$, and $\epsilon = 1.5$ to have the desired performance.

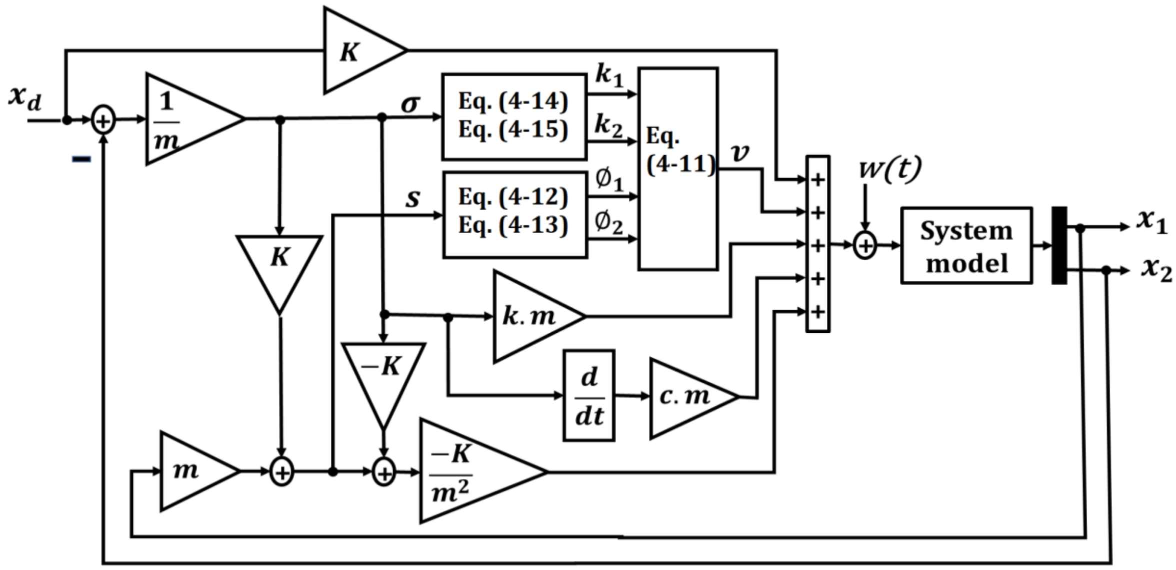

Figure 4.1: Simulink block diagram of the controller algorithm.

The system parameters are obtained from the modal tap test of the boring bar with the MR damper as shown in the frequency response function FRF in section 5.2 in the following chapter. The values when the controller is OFF are considered as the system nominal parameters that are used for controller design and simulations. The simulation responses for step and harmonic inputs are given in Figure 4.2 showing the fast response of the controlled system as the desired value can be reached in a finite time less than 30 milliseconds. Moreover, the controller with the tuned parameters was successfully tested in several cutting tests at different cutting conditions as illustrated in the next chapter.

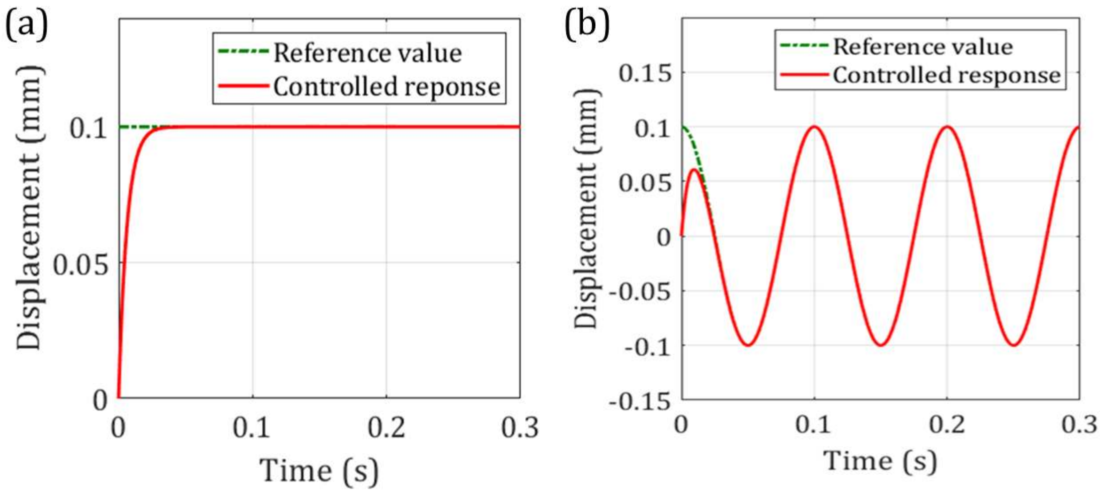

Figure 4.2: Response of the controller to (a) step input and (b) harmonic input.

To check the controller response under parametric uncertainties, the stiffness and mass values are varied around their nominal values k_o and m_o. the controller is insensitive to stiffness change as shown in Figure 4.3 (a). Variation of the modal mass from 0.7 to twice of its nominal value shows good response in this range as in Figure 4.3 (b).

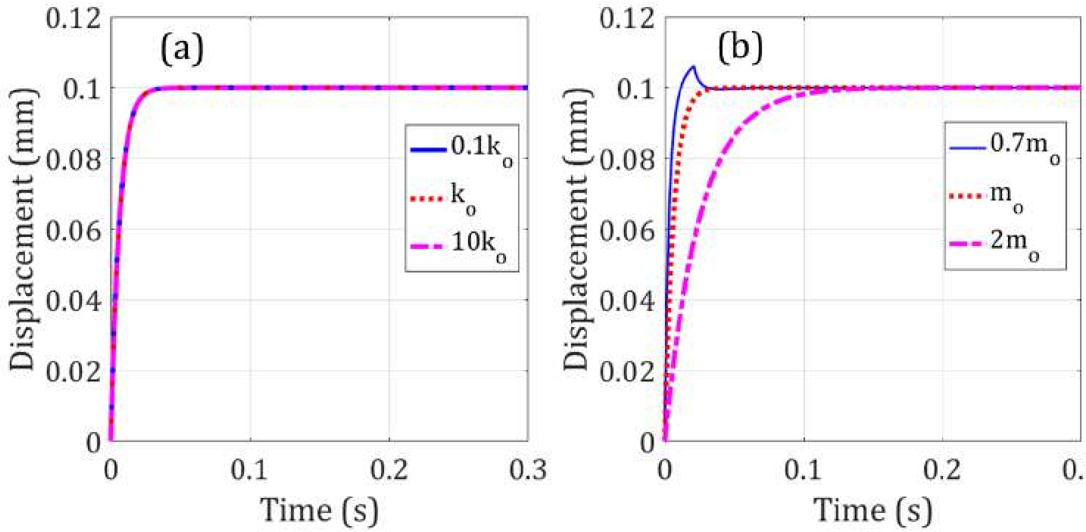

Figure 4.3: Simulation response of the proposed controller to step input with parametric uncertainties: (a) stiffness variation. (b) mass variation.

The performance of the proposed controller is compared with PID controller. The PID controller is designed to reduce the error $e(t)$ as given by Eq. (4-20). The controller parameters are tuned by using MATLAB/Simulink control toolbox, where $k_p = 10.38 \text{ x } 10^3\ N/mm$, $\tau_i = 1.1\ ms$, and $\tau_d = 0.24\ ms$. After adding a sinusoidal disturbance of 0.1 mm at frequency of 400 Hz to the system, it is clearly demonstrated in Figures 4.4(a) and 4.4(b) that the proposed controller is more robust as compared to PID controller in the presence of unmodeled dynamics. Disturbances in wider range of frequencies between 100 Hz and 1000 Hz were analyzed in terms of displacement and velocity responses as shown in Figure 4.5 and Figure 4.6, respectively. The performance of the proposed controller is better than the PID controller regarding disturbance rejection in wide frequency range.

$$u_{PID}(t) = k_p\left[e(t) + \frac{1}{\tau_i}\int e(t)dt + \tau_d\frac{de(t)}{dt}\right] \quad (4\text{-}20)$$

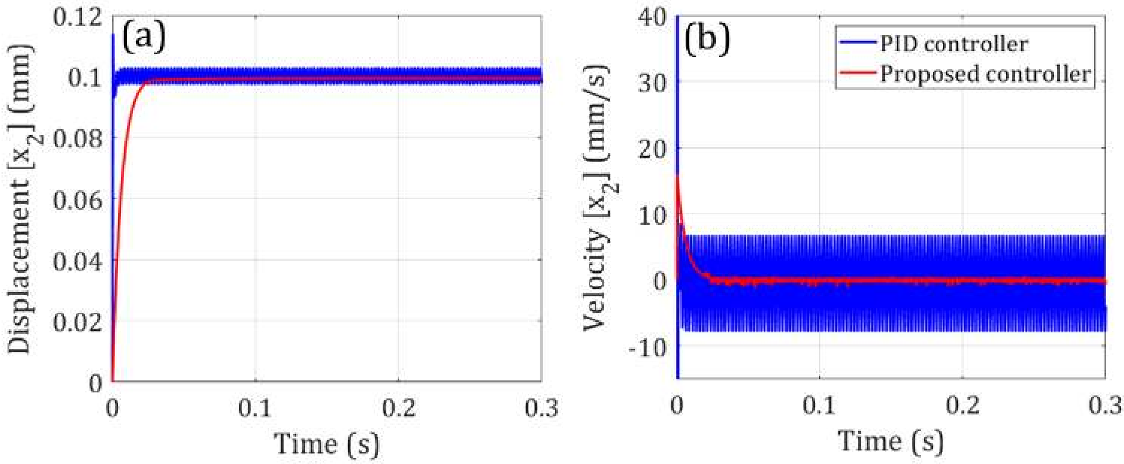

Figure 4.4: Comparison of PID and the proposed controllers for step input response with sinusoidal disturbances added to the system: (a) displacement response. (b) velocity response.

4.5 Summary

The design of a sliding mode controller utilizing the variable gain super twisting algorithm and its application to magnetorheological fluid damper for boring bars is presented in this chapter. The proposed controller offers the advantages of the classical sliding mode control while avoiding its inherent chatter problem.

Boring bar with MR damper is modeled as single degree spring-mass-damper system. The developed system is simulated in MATLAB Simulink. Simulation results showed robustness of the proposed controller against disturbances as compared to PID controller in wide range of frequencies. Moreover, the controller can compensate for parametric uncertainties in system model.

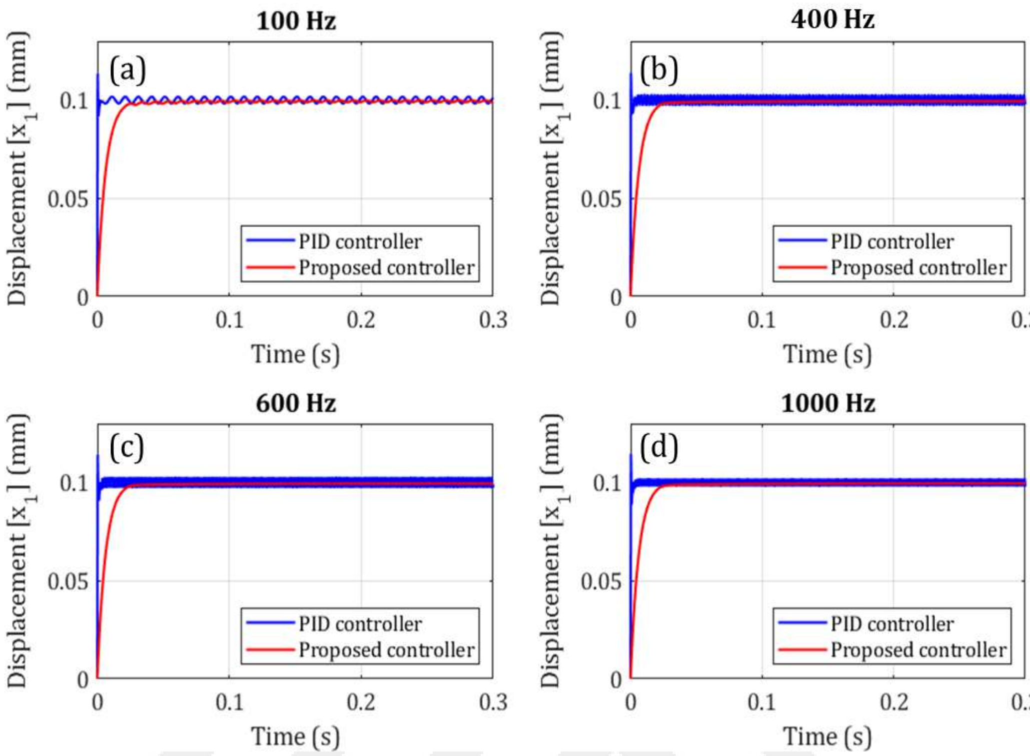

Figure 4.5: Displacement response of PID and the proposed controllers for step input with sinusoidal disturbances added to the system at different frequencies: (a) 100 Hz (b) 400 Hz (c) 600 Hz (d) 1000 Hz.

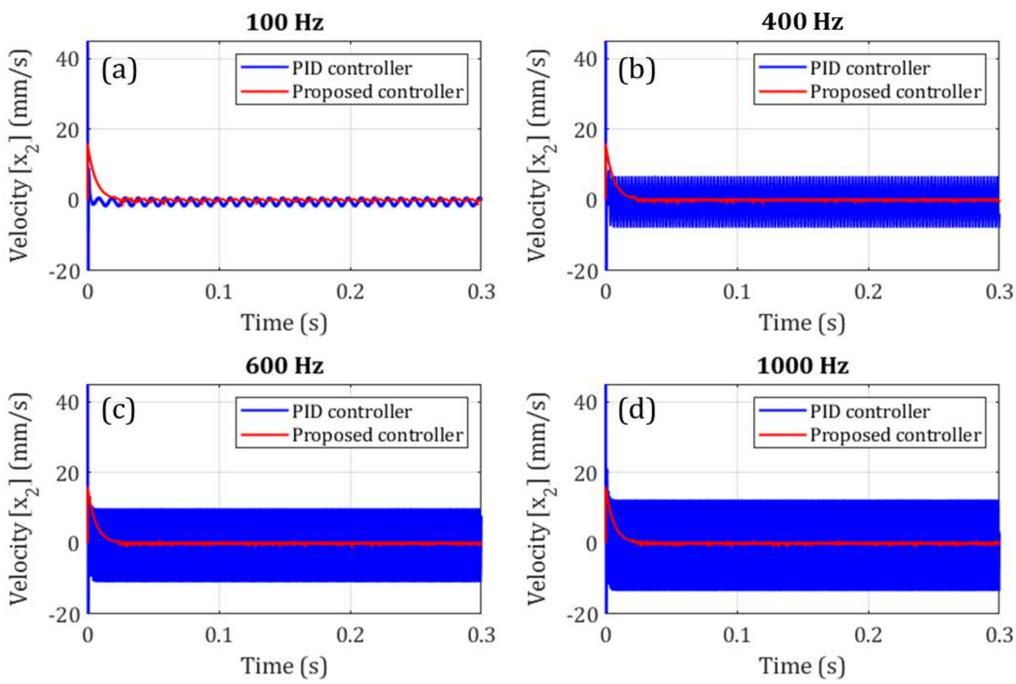

Figure 4.6: Velocity response of PID and the proposed controllers for step input with sinusoidal disturbances added to the system at different frequencies: (a) 100 Hz (b) 400 Hz (c) 600 Hz (d) 1000 Hz.

Chapter 5

EXPERIMENTAL VALIDATIONS

5.1 Overview

Experimental verification of the proposed magnetorheological damping system for boring bars is presented in this chapter. Prior to actual boring tests, many other tests were performed for identifying system parameters and material properties. Experimental setup and results of each of these tests are discussed below. Boring tests were performed on two different materials: Al7075 and Inconel 718 which are used in different aerospace applications. The effectiveness of the proposed system is shown on acceleration measurements and the surface roughness of the machined surfaces.

5.2 System Identification

5.2.1 Modal analysis

Modal analysis is a widely accepted method to experimentally identify the modal parameters of the system such as natural frequency, stiffness, damping ratio, and damping coefficient. The manufactured MR damper is installed on the CNC turning center as shown in Figure 5.1. The boring bar is excited by the impulse force hammer model 9722A500 from Kistler. The response is measured by a uniaxial accelerometer type 8774A50 from the same supplier. The accelerometer is placed 20 mm away from the tip of the bar to allow proper excitation by the hammer in the radial direction. Both the hammer and the accelerometer were connected to the data acquisition card NI-9234 and Cutpro software from MAL inc. Sampling rate of 5 kHz is used during these tests.

The tests were performed for the two commercial boring bars which were used in the cutting tests: 25T-SVUBR-16D and A25T-SCLCR-12 from Sandvik. Both the bars have the same length and diameter of 300 and 25 mm, respectively. As the proposed design of the damper allows for adjusting the overhang length of the bar according to the process requirements, the impact hammer tests were performed for the two bars at different overhang lengths.

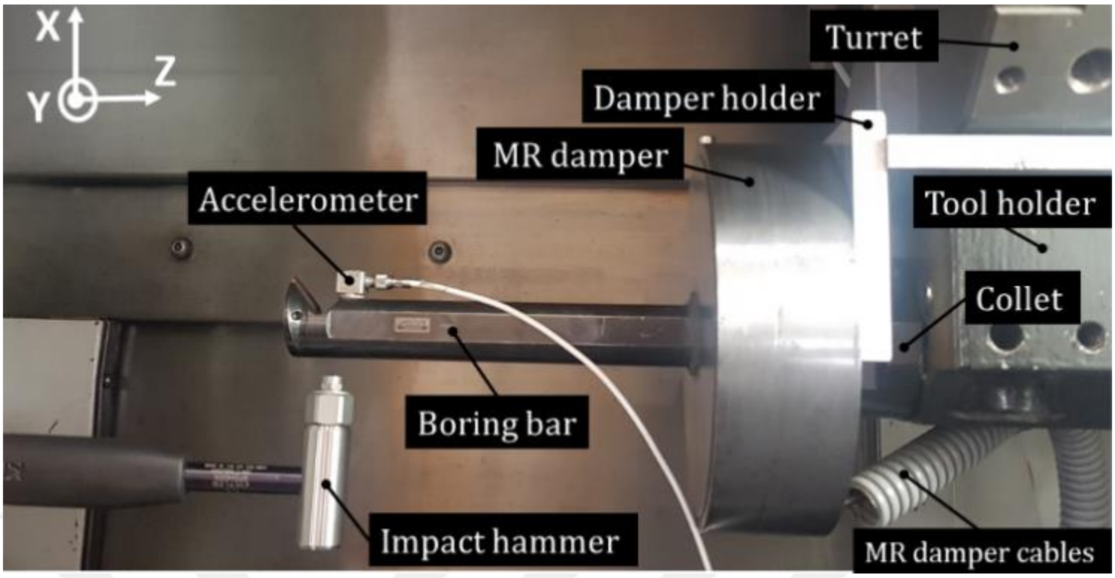

Figure 5.1: Experimental setup for the impact hammer test.

The frequency response function (FRF) plot of the first boring bar with an overhang length of 150 mm is shown in Figure 5.3, illustrating a single mode in the radial direction at a frequency of 397 Hz when the controlled system is OFF. When the MR damper is activated, the frequency increases to 436 Hz due to the slight increase in the modal stiffness. The modal parameters are given in Table 5.1, showing that the modal damping is increased by 141% by the developed system. The impact test results for the second boring bar at overhang length of 165 mm are presented on the frequency response function FRF in Figure 5.4 and the listed values in Table 5.2.

In order to compare the modal test results of the boring bar setup with and without the damper, the same bar is attached directly to the tool holder and the turret without the MR damper but at a reduced overhang length after subtracting the axial length of the damper to have the same effective length (i.e., the length that can be used inside the bore) as illustrated in Figure 5.2. This configuration is mentioned as reference tool in cutting tests results. The reduction in length results in higher stiffness of the bar but with less damping component as explained in the tabulated results. This difference in damping has a noticeable contribution to the improvement of the chatter-free depth of cut and stability of the system as shown on stability lobe diagrams which are explained in section 5.3.

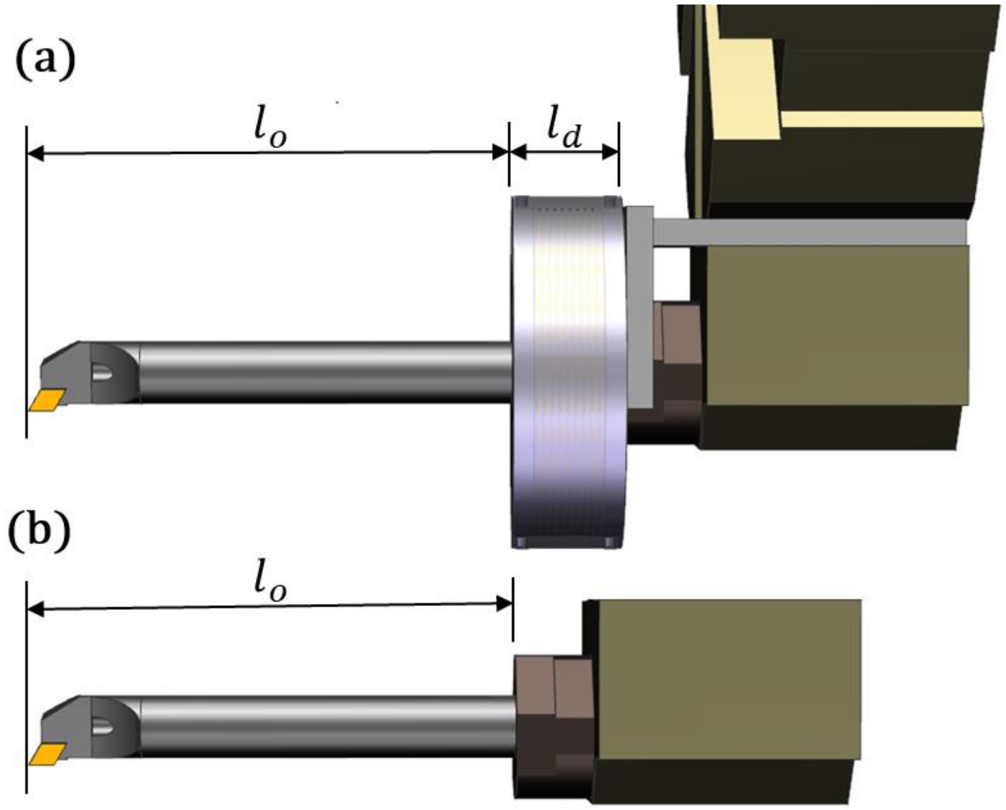

Figure 5.2: CAD figure illustrating the overhang length (a) with MR damper, (b) reference tool without damper.

Table 5.1: Modal parameters of the boring bar 25T-SVUBR-16D at overhang length of 150 mm.

Parameter	MR controller OFF	MR controller ON	Without MR damper
Frequency (Hz)	397	436	621
Modal Damping (%)	6.1	14.7	1.4
Modal Stiffness (N/mm)	1405	1726	3738

Table 5.2: Modal parameters of the boring bar A25T-SCLCR-12 at overhang length of 165 mm.

Parameter	MR controller OFF	MR controller ON	Without MR damper
Frequency (Hz)	356.5	357.3	527.5
Modal Damping (%)	3.4	10.7	2.3
Modal Stiffness (N/mm)	1416	1526	3950

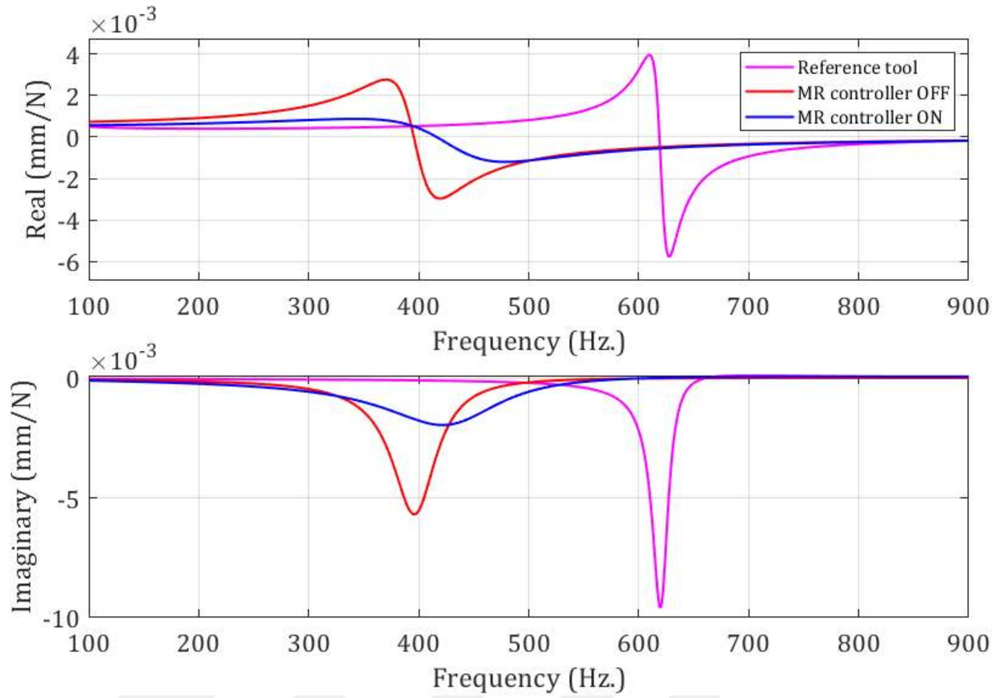

Figure 5.3: FRF of the boring bar 25T-SVUBR-16D in the radial direction at overhang length of 150 mm with MR controller ON and OFF and reference tool.

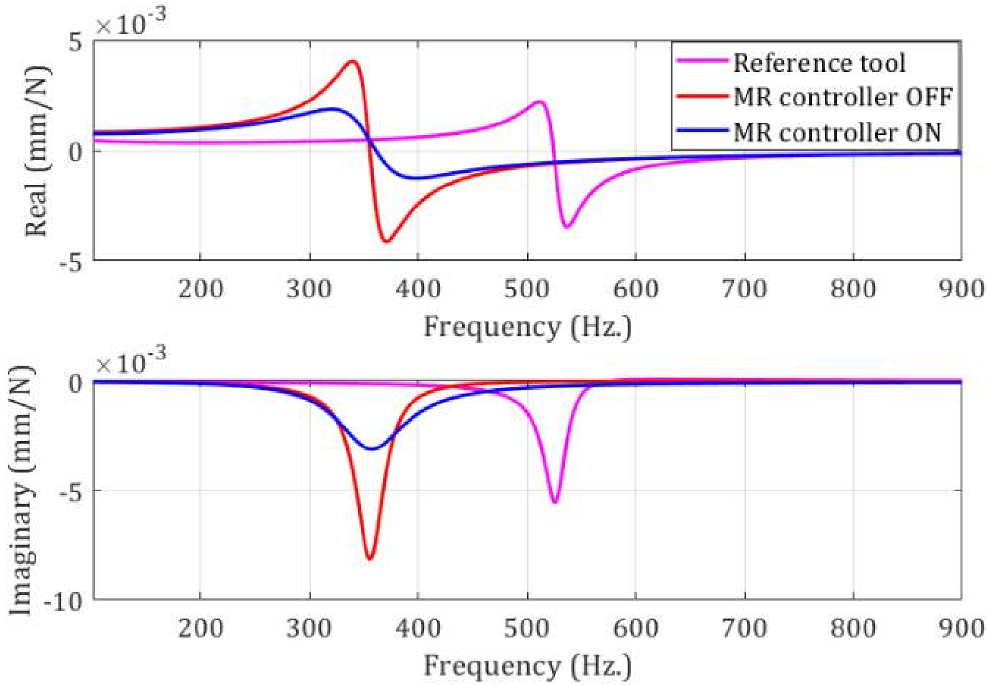

Figure 5.4: FRF of the boring bar A25T-SCLCR-12 in the radial direction at overhang length of 165 mm with MR controller ON and OFF and reference tool.

5.2.2 Orthogonal calibration tests

Orthogonal calibration is a two-dimensional cutting operation in which the cutting edge is perpendicular to the direction of cutting velocity. This process is used to identify the material properties such as shear stress and shear angle which are widely varied from the values obtained by classical tensile tests because of high shear rates during machining operations. The obtained results are then processed with insert geometrical parameters to obtain the cutting coefficients in the three cutting directions through oblique transformation procedure (Altintas, 2012).

The orthogonal calibration tests were performed on the two workpiece materials which were used for the boring tests Inconel 718 and Al 7075. The setup for orthogonal cutting test is shown in Figure 5.5. the cutting insert is attached to the table type dynamometer which is used to measure the cutting forces in the three perpendicular directions. The force signals are transferred to the charge amplifier and converted into digital signals through DAQ card NI-6259.

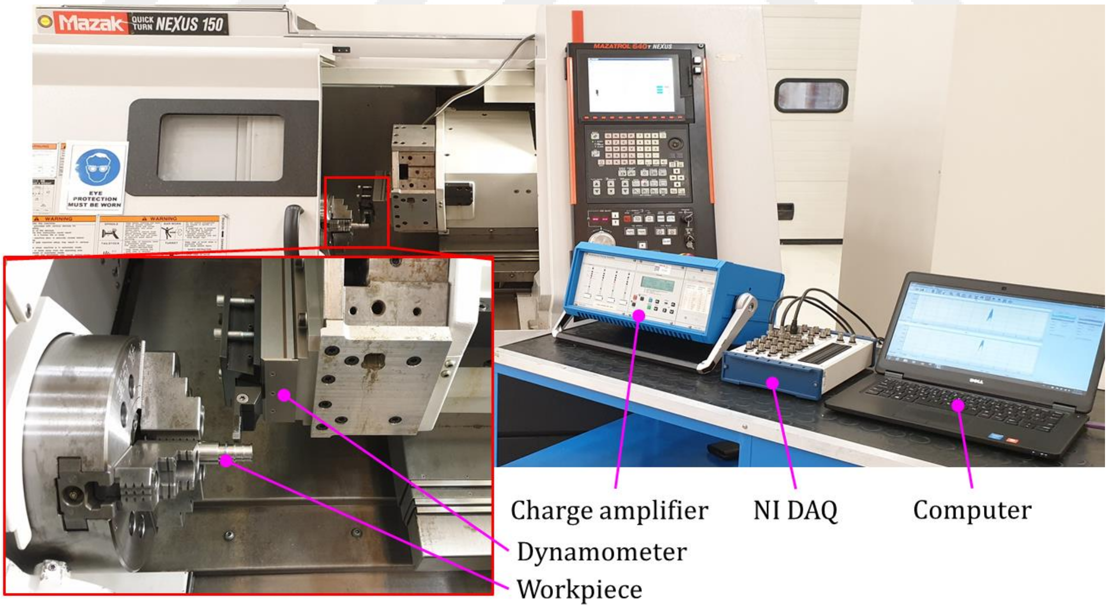

Figure 5.5: Orthogonal calibration test setup

As the shear stress values are affected by the shear rate, the calibration tests should be performed at cutting speeds close to the values that will be used during boring experiments.

For this reason, orthogonal tests were performed at cutting speed of 200 m/min for Al7075 workpiece and at 30 m/min for Inconel 718, both were performed without coolant. The average cutting forces are calculated and plotted against the uncut chip thickness which is determined by the feedrate in the radial direction. The chips are collected after each test for measuring their average thickness and calculate the average chip ratio.

Average tangential and feed forces are plotted versus feed rate values as shown in Figures 5.6 and 5.7 for both workpieces. Average shear stress of 841 MPa, along with average shear and friction angles of 27.8° and 36.4° were obtained for Inconel 718 workpiece. The calibration tests of Al 7075 workpiece results in an average shear stress of 351 MPa, and average shear and friction angles of 38.6° and 25.6°, respectively.

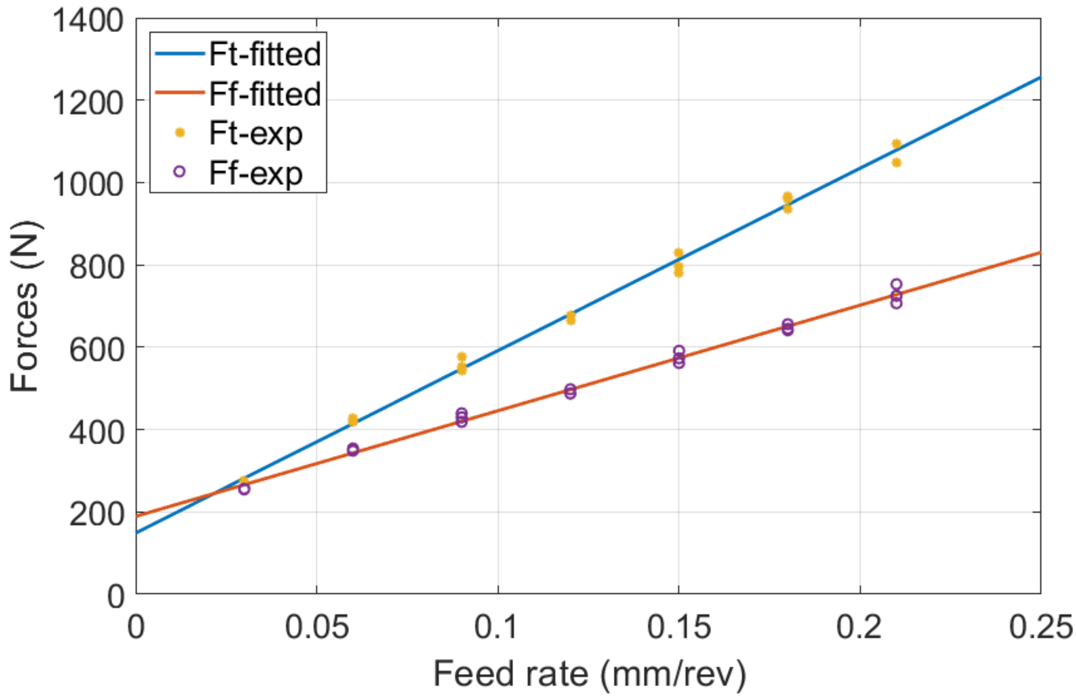

Figure 5.6: Orthogonal cutting forces against feedrate for Inconel 718 workpiece.

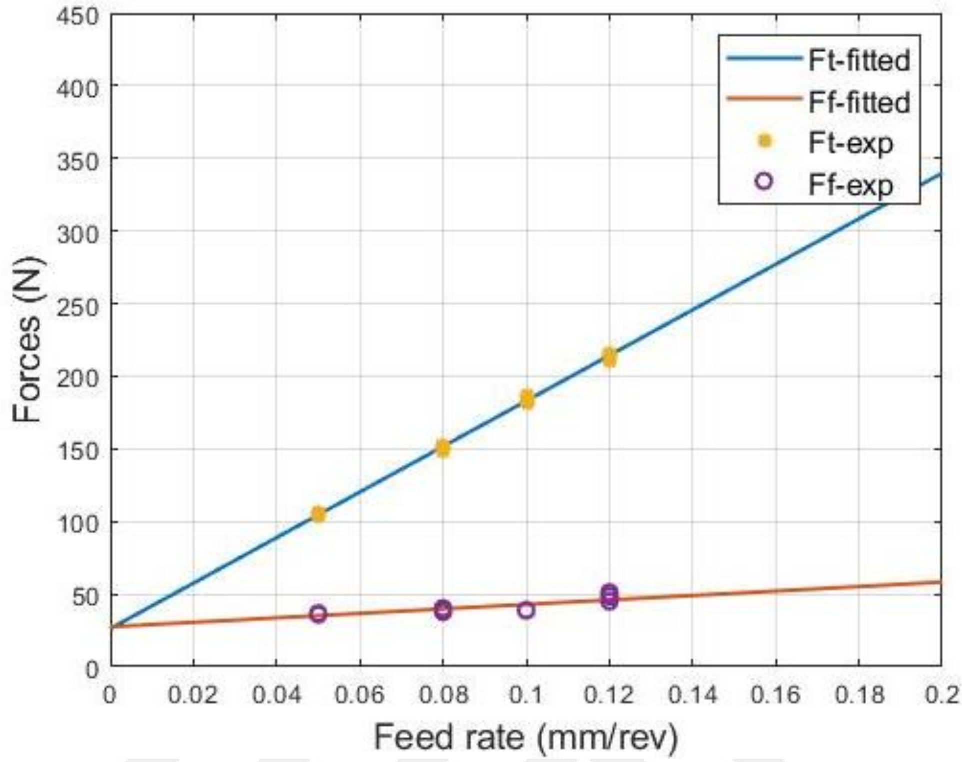

Figure 5.7: Orthogonal cutting forces against feedrate for Al7075 workpiece.

5.3 Stability lobe diagrams

Stability lobe diagrams are very useful criteria to determine the machining parameters by locating the cutting point in one of the stable pockets at high spindle speeds with high depth of cut to increase the productivity of the process. In contrast to milling operations where high spindle speed can be achieved, boring operations are performed at relatively lower rotational speed and utilize single cutting point tools. Due to that, stability lobes become very narrow, and it is difficult to determine a stable point between the many intersecting lines, hence the absolute stability limit (i.e., the straight line crossing the lowest peaks of all the lobes on the diagram) becomes more reliable. Increasing this limit will enhance the productivity of the boring process. The basic model for stability lobe diagrams is developed by Tlusty and Polacek (1963) as represented by Eq. (5-1). It shows that stability limits are inversely proportional to the cutting coefficient in the chip thickness direction K_f and the real part of the transfer function $Re[G(\omega)]$. Increasing stiffness and damping of the system greatly helps in raising the absolute stability limit by minimizing the absolute value of the negative real part of the transfer function as explained in Eq. (5-2) (Altintas and Weck, 2004). Enhancements of damping and stiffness due to the proposed system increase stability limits of the boring process.

$$b_{lim} = -\frac{1}{2K_f Re[G(\omega)]} \tag{5-1}$$

$$\min(Re[G(\omega)]) = -\frac{1}{4k\zeta} \tag{5-2}$$

The effect of the developed damping system on stability lobe diagrams can be illustrated by Figure 5.8. Activating the MR damper increases the stiffness and the damping of the system which results in increasing the stability limit. An example of the created stability lobes and the absolute stability limits for boring of the Inconel 718 workpiece with a boring bar at an overhang length of 150 mm is given in Figure 5.8. Installing the MR damper without activation increases the limit from 0.05 to 0.09 mm because of the viscous damping of the MR fluid while it is in the off state; however, activating the damper increases the absolute stability limit to 0.23 mm at the given length. This increase in stability limits is further validated by experimental boring tests as presented in the next section.

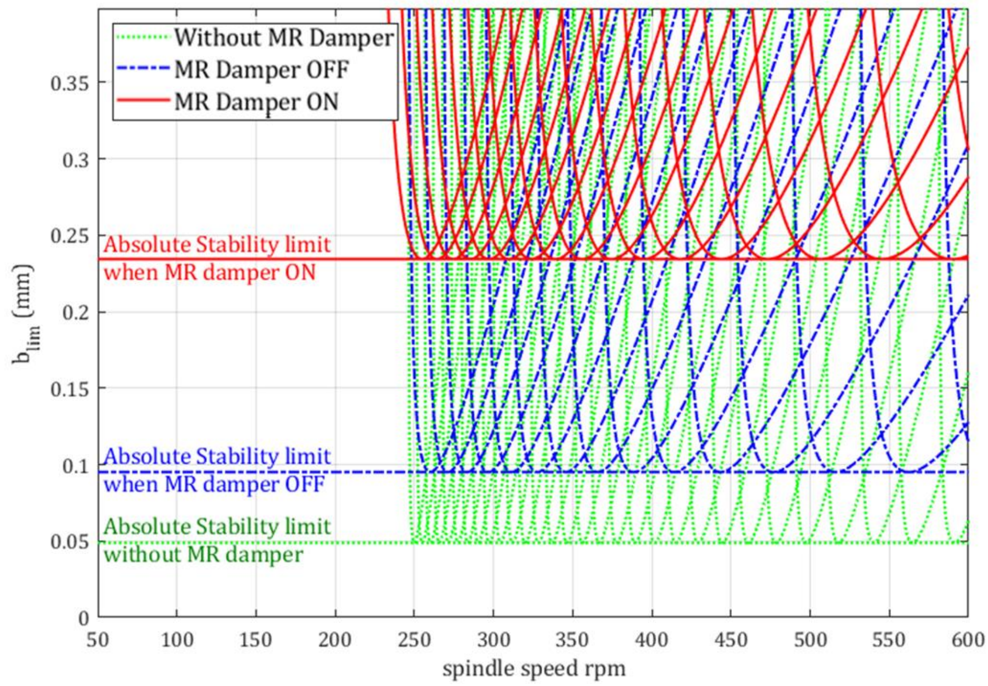

Figure 5.8: Effect of the developed system on stability lobe diagrams and stability limits for boring Inconel 718 workpiece with bar at an overhang length of 150 mm.

5.4 Boring test results

The boring bar with the MR damper was installed on the CNC turning center as shown in Figure 5.9. A uniaxial accelerometer is placed 30 mm away from the insert tip to measure the acceleration of the boring bar in the radial direction during cutting tests. The measured acceleration is fed to the controller via DAQ card NI-6259. The acquired acceleration signal is integrated and fed to the controller. The controller output signal is sent to the analog output of the DAQ card in terms of a pulse width modulated PWM signal that drives the required current from the DC power supply. A low pass filter of 1kHz cutoff frequency is used to avoid excitation of any unexpected higher modes during the controller implementation. Cutting tests were performed on two different materials with two different boring bars at variable overhang length.

5.4.1 Al 7075 boring tests

The cutting tests were performed on Al7075 workpieces with outer and inner diameters of 150 and 100 mm, respectively. The MR damper is integrated to a commercial boring bar A25T-SCLCR 12 with 0.8 mm nose radius insert CCGX 04-08-Al from Sandvik. The overhang length l_o is set to 165 mm from the insert to the face of the damper. Since the damper itself has an axial length of 43 mm, this extended length add compliance to the boring bar in the OFF state. Activating the damper in the controller ON case improves the stiffness and stability of the system; however, this comparison is not fair as the stiffness of the system was already reduced prior to adding the controlled damping effect. For this reason, the developed system is compared with a reference tool which is the same boring bar but attached directly to the collet and the tool holder at the same overhang length of 165 mm without the MR damper as explained in Figure 5.2.

Figure 5.10 shows the measured acceleration results with their frequency spectrum for one of Al7075 boring tests with MR controller ON and OFF. The comparison between the MR controlled system and the standard reference tool for the same cutting conditions is given in Figure 5.11. The cutting conditions of the presented results are 100 mm bore diameter, 200 m/min cutting speed, 10 μm/rev feedrate, and 0.1 mm radial depth of cut.

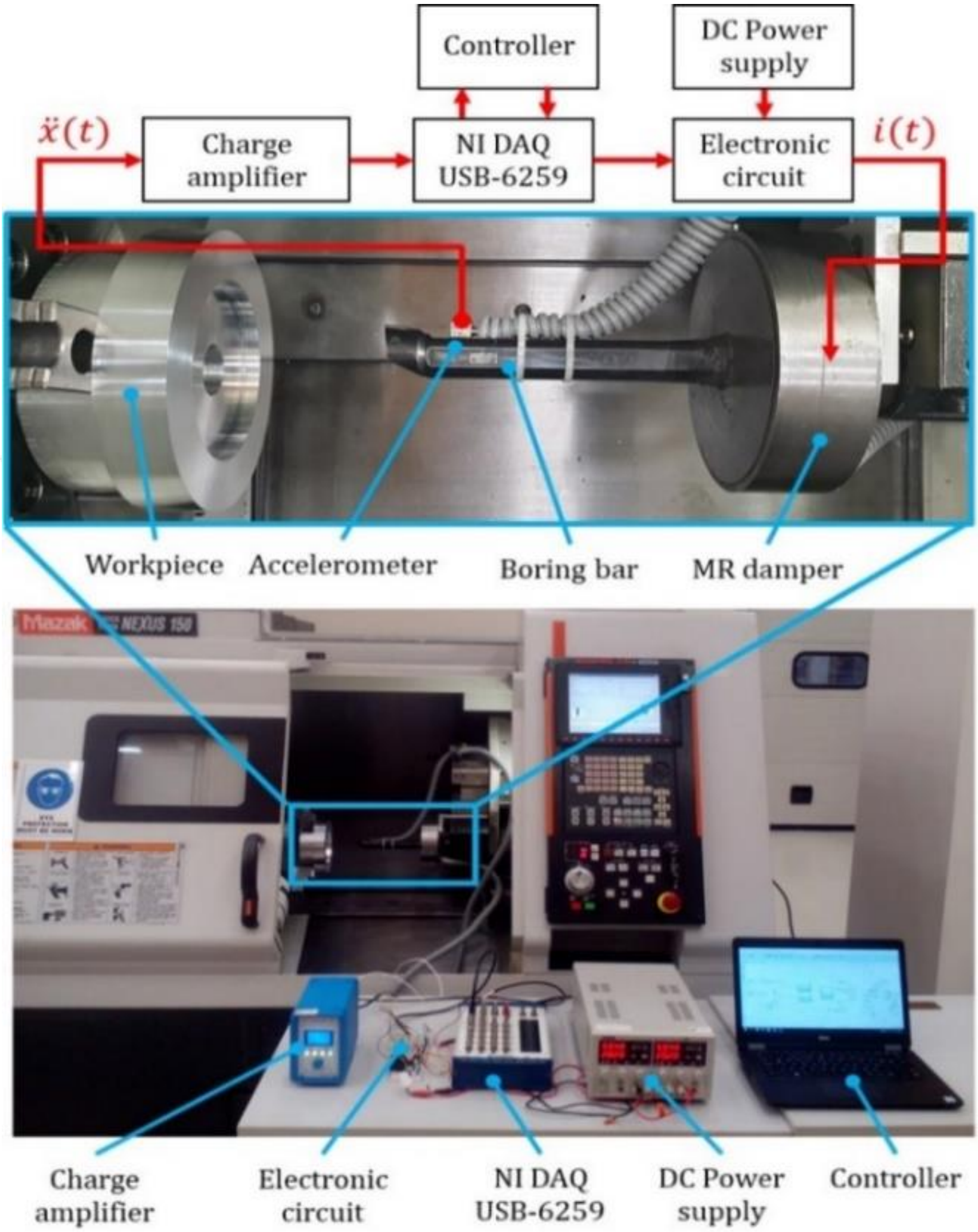

Figure 5.9: Experimental setup for the boring bar with the MR damper on the CNC turning center.

It is clearly shown that acceleration measurements of the MR controlled system have stable signals with attenuated acceleration values compared to both the controller OFF case and the reference tool. Moreover, the frequency response spectrum of the measured signals shows that the measured signal at the chatter frequency is effectively suppressed by the developed MR controlled system in both cases.

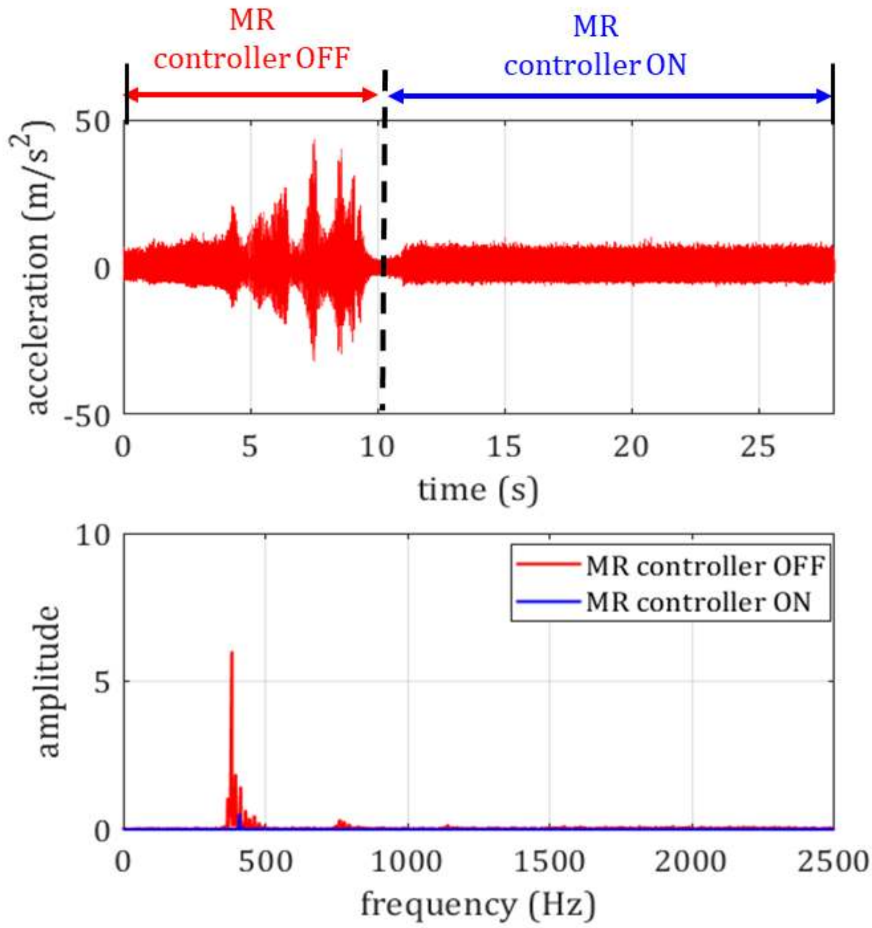

Figure 5.10: Measured acceleration in the time domain and its Frequency spectrum with MR controller OFF and ON for boring Al7075 workpiece with bar at overhang 165 mm, spindle speed: 640 rpm, feedrate: 0.01 mm/rev, radial depth of cut: 0.1 mm.

To verify the effect of the controlled system on the stability limits, several boring tests were performed under different machining conditions with both MR controlled boring bar and the standard reference tool. The presented results in Figure 5.12 show the increase of the absolute stability limit for the radial depth of cut (b_{lim}) from 30 microns to 100 microns for the Al7075 workpiece at the given overhang length of the boring bar.

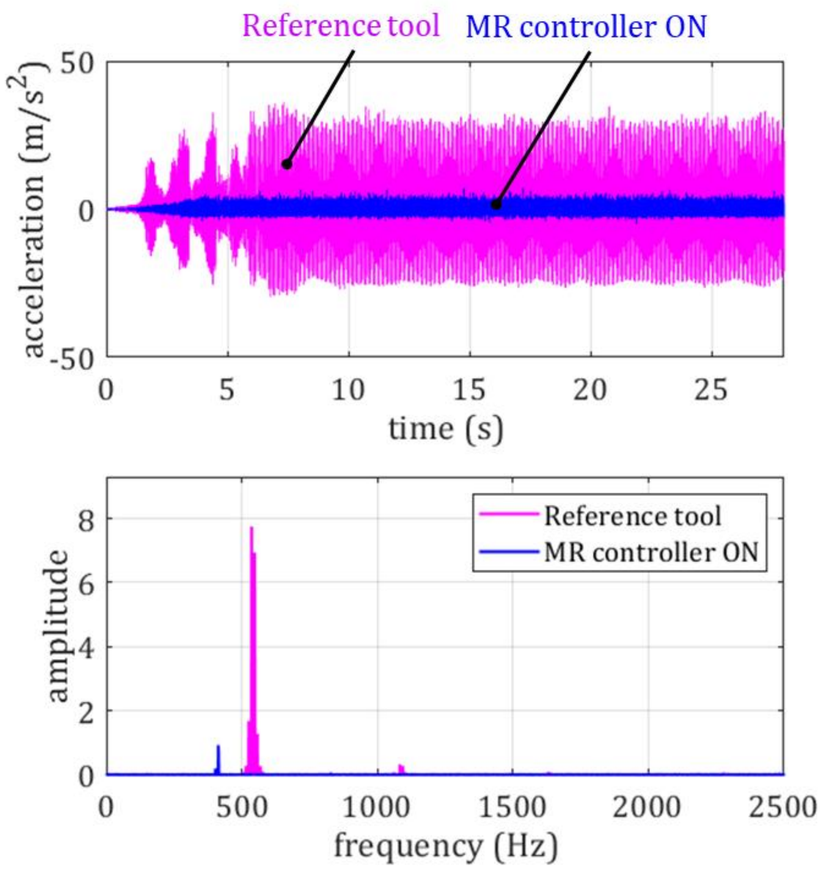

Figure 5.11: Measured acceleration in the time domain and its frequency spectrum MR controlled bar and reference tool for boring Al7075 workpiece with bar at overhang 165 mm, spindle speed: 640 rpm, feedrate: 0.01 mm/rev, radial depth of cut: 0.1 mm.

The surface roughness measurements for tests at different depths of cut are presented in Table 5.3. Surface roughness values significantly improve about 3 to 5 times with the developed MR controlled system compared to the reference boring tool. Moreover, the quality of the machined surfaces can be visually inspected as shown in Figure 5.13.

Table 5.3: Surface roughness measurements for Al7075 workpiece.

Depth of cut:	50 µm		100 µm	
	Reference tool	MR Controller ON	Reference tool	MR Controller ON
R_a (µm)	1.92	0.65	5.74	1.12
R_z (µm)	9.08	3.09	26.56	5.45

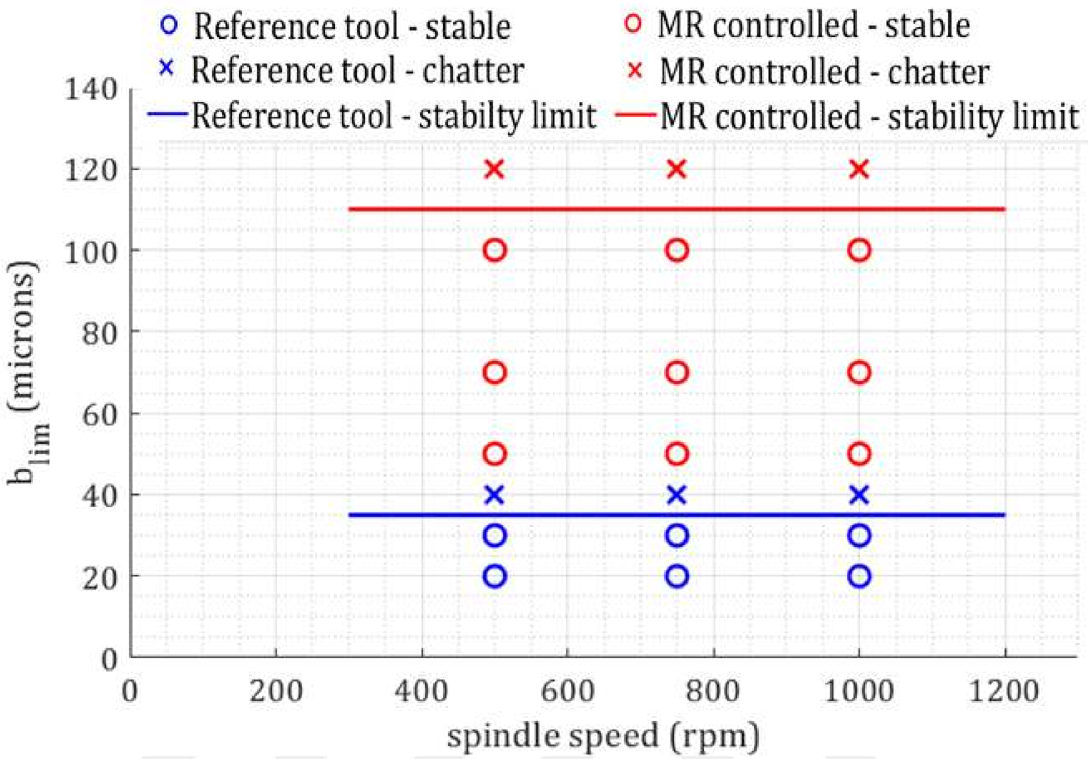

Figure 5.12: Stability limits improvements by the MR controlled boring process for Al7075 workpiece with boring bar at overhang length of 165 mm.

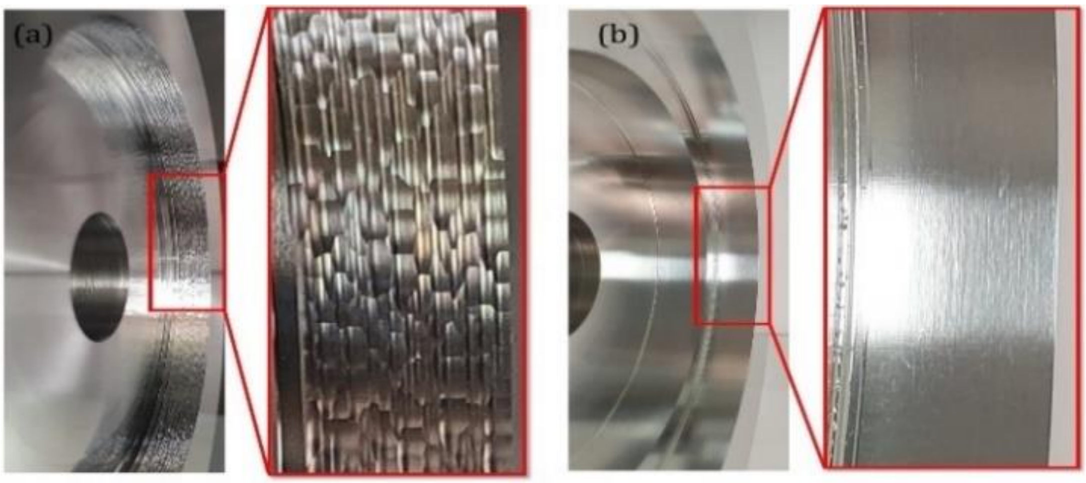

Figure 5.13: Illustration of bored surfaces of Al7075 workpieces: (a) chatter when MR controller OFF and (b) stable cut when MR controller ON– bore diameter: 100 mm, cutting speed: 200 m/min, feedrate: 10 µm/rev, radial depth of cut: 100 µm.

As the damper allows for adjusting the overhang length, more tests were performed at different overhang length and consequently different natural frequencies. Modal parameters of the boring bar at overhang length of 130 mm are shown in table 5.4. Figure 5.14 shows acceleration test results for cutting Al7075 workpiece by the boring bar at the given overhang length. Acceleration measurements demonstrated that the new MR damping system can effectively damp the chatter vibrations at these different conditions as shown on both time and frequency domain results. The quality of the bored surfaces is investigated as shown on Figure 5.15.

Table 5.4: Modal parameters in the radial direction at an overhang length of 130 mm.

Parameter	MR Damper OFF	MR Damper ON	Without MR damper
Frequency (Hz)	719	801	869
Modal Damping (%)	4.1	9.6	0.65
Modal Stiffness (N/mm)	4561	5799	7857

5.4.1 Inconel 718 boring tests

To verify the effectiveness of the proposed system on different workpiece material, several boring tests were performed on Inconel 718 workpiece. As the designed damper allows for changing boring bars, another boring bar model 25T-SVUBR-16D from Sandvik is used for Inconel tests. The bar has diameter of 25 mm, and the overhang length is set to be 150 mm. The used insert has 0.4 mm nose radius, 93^{o} approach angle, and a rhombic shape of 35^{o} point angle. This small point angle is selected to minimize the effect of the insert geometry on producing vibrations.

Several boring tests were performed on the Inconel 718 workpiece at different cutting depths from 0.05 to 0.25 mm and at cutting speeds of 25, 30, 35, and 40 m/min without coolant, for both controller ON and OFF conditions of the MR damper in addition to the reference standard tool at same overhang length.

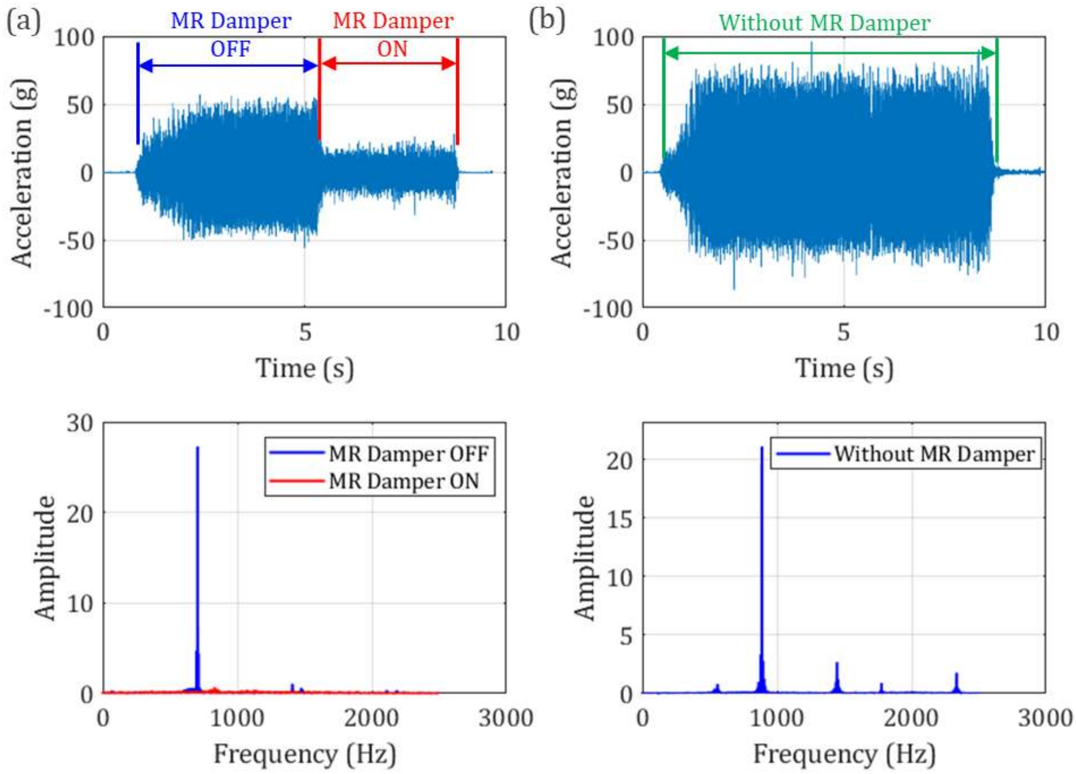

Figure 5.14: Measured acceleration in the time domain and its frequency spectrum for the boring test of Al 7075 workpiece: (a) MR damper on and off. (b) without MR damper (Boring conditions: overhang length of 130 mm, spindle speed of 500 rpm, feedrate of 0.3 mm/rev, radial depth of cut of 0.3 mm).

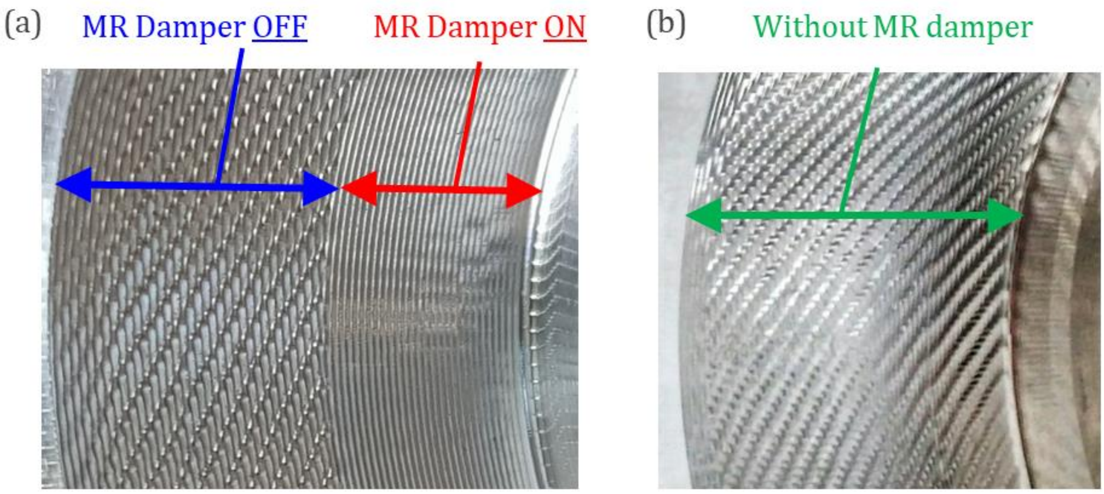

Figure 5.15: Illustrations of the bored part surfaces of Al 7075 part with and without MR damper: (a) MR damper on and off. (b) without MR damper (boring conditions: overhang length of 130 mm, spindle speed of 500 rpm, feedrate of 0.3 mm/rev, radial depth of cut of 0.3 mm).

The results, as presented on the stability lobe diagrams in Figure 5.16, point the increase of the absolute stability limit from 0.09 to 0.23 mm by activating the MR damper at the given boring length. While several other boring tests were also performed at speeds lower than 25 m/min, their results are not included, as they showed higher stability limits even without activating the damper due to the process damping effect which is not considered in the current work.

The acceleration results and their frequency spectrum for two Inconel boring tests with and without the MR damper under the same cutting conditions are given in Figure 5.17. It shows that chatter vibrations are successfully damped with the aid of the proposed MR damping system. Furthermore, the improvements on the quality of the machined surfaces of the two tests are presented in Figure 5.18. The Boring conditions of the presented tests are as follows: overhang length of 150 mm, spindle speed of 320 rpm, feedrate of 0.1 mm/rev, and radial depth of cut of 0.2 mm.

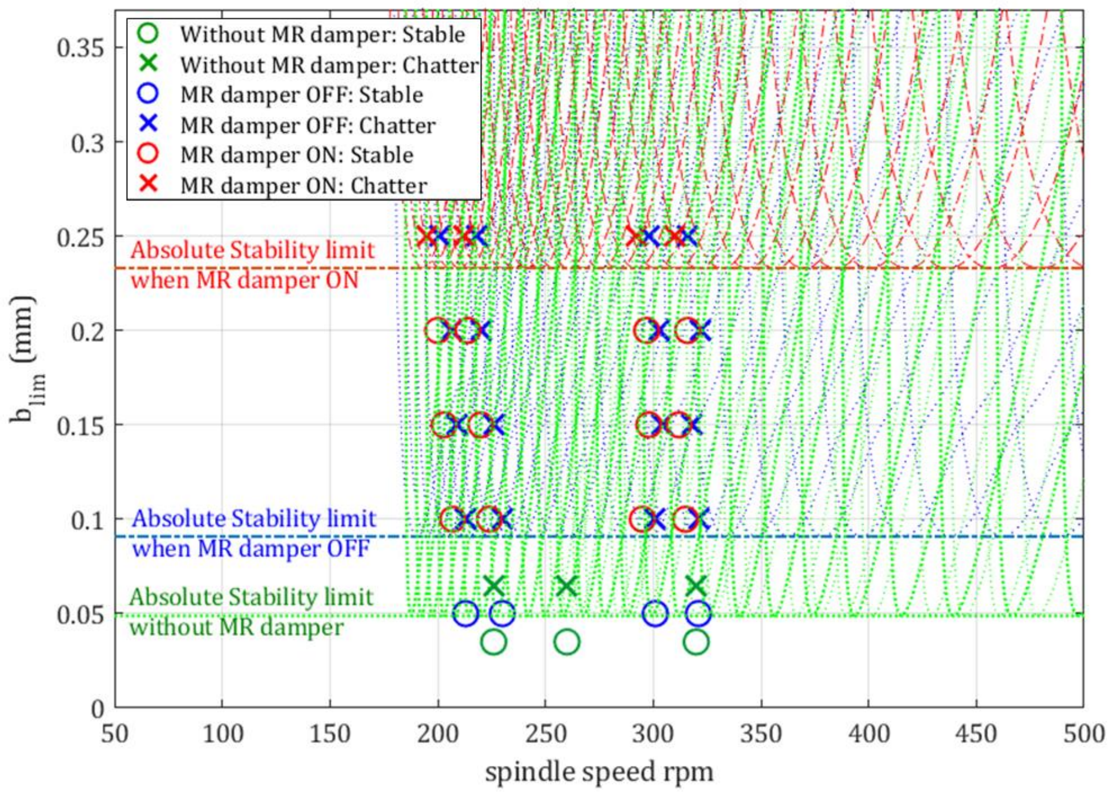

Figure 5.16: Illustration of the cutting test points on the stability lobe diagrams for boring of Inconel 718 workpiece.

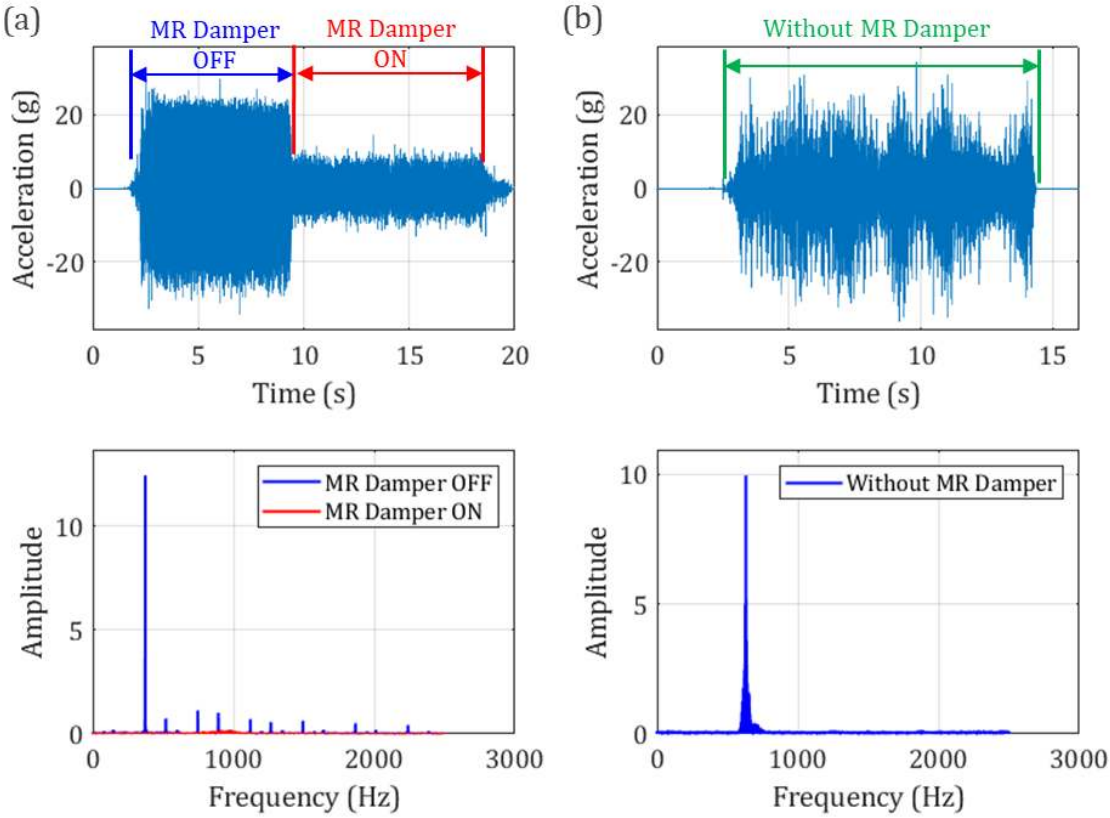

Figure 5.17: Measured acceleration in the time domain and its frequency spectrum for one of Inconel 718 boring tests: (a) MR controller ON and OFF. (b) without MR damper.

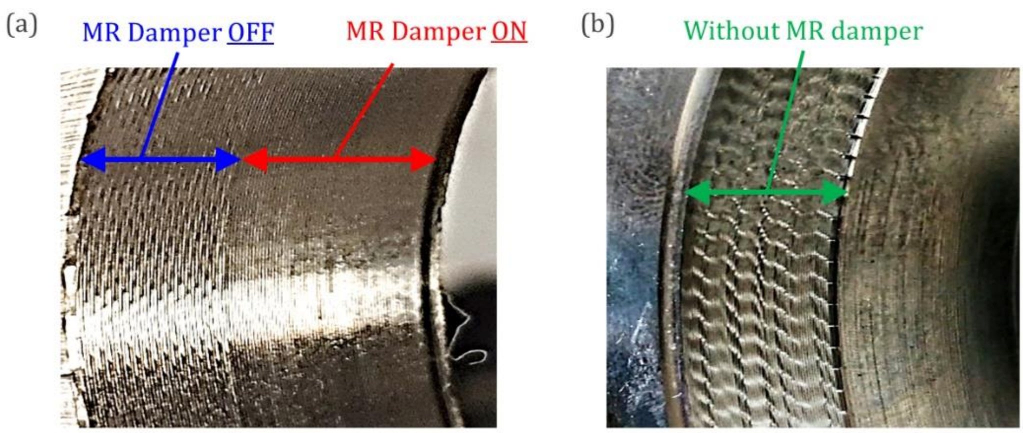

Figure 5.18: Illustrations of the quality of the bored surfaces of Inconel 718 workpiece: (a) MR controller ON and OFF. (b) without MR damper.

5.5 Comparison with available literature results

In this section, the developed system is compared with available literature results. Two main factors were used for the comparison: the real part of the FRF which indicates the enhancements in damping and dynamic stiffness, and the absolute stability limit as given in Table 5.5 and Table 5.6, respectively. Since cutting conditions and geometrical parameters of the boring bar are different for each research work, comparison was made in terms of percentage change of each parameter. As shown in Table 5.5, improvement ratio of 70% were achieved in this work for the bar at overhang length of 165 mm. This ratio is higher than the other two ratios of Biju and Shunmugam, (2018) and Yigit et al., (2017). The ratio is close to that of Lu et al., (2014); however their reported values are for the magnitude of the FRF not only the real part. Some other literature results were reported only in terms of absolute stability improvements as mentioned in Table 5.6 without referring to the improvements in the FRF.

Table 5.5: Comparison of FRF real part improvements

Research work	Technology	Min Real Part of FRF (m/N)		
		Uncontrolled	Controlled	Improvement ratio
Current work	MR fluid	-4.114 E-06	-1.247E-06	70%
Biju and Shunmugam, (2018)	MR fluid	84.45E-06[a]	41.4E-06[a]	51%
Yigit et al., (2017)	Piezoelectric actuator	-22.6E-06	-11.6E-06	49%
Lu et al., (2014)	Magnetic actuator	24.08E-06[b]	6.82E-06[b]	72%

a: values of real part is calculated based on reported values of stiffness and damping.
b: These are the magnitude values of the FRF at frequency of 1265 Hz. as real and imaginary parts were not reported separately.

Improving damping and dynamic stiffness affects the real part of FRF which is inversely proportional to the absolute stability limit; however, there are other factors that contributes to stability limit such as insert geometry, approach angle, and the ratio between insert nose radius and radial depth of cut as reported by (Ozlu and Budak, 2007a). This illustrates that the ratios in Table 5.6 are not exactly the inverse of the reported ratios in Table 5.5.

For absolute stability limit improvements, the proposed system shows better performance than the available ratios of other MR fluid devices. Although the achieved results is less than the ratios obtained by other techniques as reported by Yigit et al., (2017) and Lu et al., (2014), the proposed system has other advantages regarding the size of the actuating device and its easy installation procedure.

Table 5.6: Comparison of absolute stability limit improvements

Research work	Technology	Absolute stability limit (mm)		
		Uncontrolled	Controlled	Improvement ratio
Current work	MR fluid	0.03	0.1	233.3%
Biju and Shunmugam, (2018)	MR fluid	0.1	0.2	100%
Som et al., (2015)	MR fluid	0.5	1.5	200%
Yigit et al., (2017)	Piezoelectric actuator	0.05	0.175	250%
Lu et al., (2014)	Magnetic actuator	0.03	0.12	300%

5.6 Summary

In this chapter, different experimental setups and cutting tests were presented. Modal tap tests were performed for two different boring bars at variable overhang lengths to determine the modal parameters for both controller ON and controller OFF cases, in addition to the standard reference tool at same overhang length for the sake of comparison. The modal parameters for the MR controller OFF are considered as the nominal values of the system that are used for controller design.

The other identification test is the orthogonal calibration which is used to determine the material properties such as shear stress, shear angle, and friction coefficient. Orthogonal tests were performed on two different materials Al7075 and Inconel 718. The calibration results were performed to determine the cutting coefficients which were used along with the modal analysis results to draw the stability lobe diagrams and to define the absolute stability limits.

Several boring tests were performed under different machining conditions for the two workpiece materials. The improvements due to the proposed system were successfully addressed in terms of acceleration measurements in both time and frequency domains in addition to the quality of the machined surfaces and surface roughness measurements.

Chapter 6

CONCLUSIONS

This thesis introduces a new active system for improving stability of the boring process based on magnetorheological fluid damper and sliding mode control. The proposed damper utilizes a sponge layer filled with 15 ml of a custom made bidisperse MR fluid and wrapped around the boring bar to keep the fluid in the required zone with fewer sealing requirements. The bidisperse MR fluid has good rheological properties and low sedimentation rate of the magnetic particles. The damper is designed to easily fit onto CNC turning center to improve the boring stability in higher depths of cut for the existing commercial boring bars. This design allows for an easy assembly of the boring bar and adjustment of its overhang length for different boring operations.

A new sliding mode control algorithm is designed for the boring bar with the developed MR damper. The controller is based on the variable gain super twisting algorithm, in which the chatter vibrations are considered as disturbances to the system. The controller demonstrated robustness against disturbances in a wide frequency range. Simulation results showed that the novel control algorithm drives the states of the system to the desired values in a finite time despite the existence of disturbances. This algorithm avoids the discontinuity problem of the classical sliding mode control. Moreover, the developed controller can tolerate parametric uncertainties while ensuring system stability.

The developed system was experimentally tested with two commercial boring bars on boring of Al7075 and Inconel 718 workpieces. Improvements on damping and dynamic stiffness of the bar were addressed using experimental modal analysis. The cutting test results showed significant increase in chatter-free depth of cut for both the materials while using different overhang length and various machining conditions. Acceleration measurements on both time and frequency domains showed the effectiveness of the developed damping system. In addition to that, the quality of the machined surfaces is examined visually and with surface roughness measurements.

The promising results of the developed system encourage us to further extend this approach and explore the required modifications to cover many other machining applications especially when the damping is required on the rotating side of the machine tool such as spindle of milling tool or clamping chuck of thin-wall workpieces in turning and boring operations.

Other factors that need more investigations for the developed system is the accumulated heat during long-time operations and its effect of the performance of the MR fluid and its damping properties. Also, some research can be done on the fluid filled foam layer in terms of its filling capacity and optimized fluid to foam ratio to have minimum amount of MR fluid for the highest performance of the device.

BIBLIOGRAPHY

Abele, E., Haydn, M., Grosch, T., 2016. Adaptronic approach for modular long projecting boring tools. CIRP Annals - Manufacturing Technology 65, 393–396. https://doi.org/10.1016/j.cirp.2016.04.104

Altintas, Y., 2012. Manufacturing Automation: Metal Cutting Mechanics, Machine Tool Vibrations, and CNC Design. Cambridge University Press.

Altintaş, Y., Budak, E., 1995. Analytical Prediction of Stability Lobes in Milling. CIRP Annals - Manufacturing Technology 44, 357–362. https://doi.org/10.1016/S0007-8506(07)62342-7

Altintas, Y., Weck, M., 2004. Chatter stability of metal cutting and grinding. CIRP Annals - Manufacturing Technology 53, 619–642. https://doi.org/10.1016/S0007-8506(07)60032-8

Atabey, F., Lazoglu, I., Altintas, Y., 2003. Mechanics of boring processes - Part I. International Journal of Machine Tools and Manufacture 43, 463–476. https://doi.org/10.1016/S0890-6955(02)00276-6

Biju, C. V., Shunmugam, M.S., 2018. Development of a boring bar with magneto rheological fluid damping and assessment of its dynamic characteristics. JVC/Journal of Vibration and Control 24, 3094–3106. https://doi.org/10.1177/1077546317700715

Cao, H., Zhou, K., Chen, X., Zhang, X., 2017. Early chatter detection in end milling based on multi-feature fusion and 3 σ criterion 4387–4397. https://doi.org/10.1007/s00170-017-0476-x

Carlson, J.D., Jolly, M.R., 2000. MR fluid, foam and elastomer devices. mechatronics 10, 555–569.

Chen, F., Lu, X., Altintas, Y., 2014. A novel magnetic actuator design for active damping of machining tools. International Journal of Machine Tools and Manufacture 85, 58–69. https://doi.org/10.1016/j.ijmachtools.2014.05.004

Chrzan, M.J., Carlson, J.D., 2001. <title>MR fluid sponge devices and their use in vibration control of washing machines</title> 4331, 370–378. https://doi.org/10.1117/12.432719

Eynian, M., Altintas, Y., 2009. Chatter stability of general turning operations with process damping. Journal of Manufacturing Science and Engineering, Transactions of the ASME 131, 0410051–04100510. https://doi.org/10.1115/1.3159047

Fallah, M., Moetakef-imani, B., 2019. Design , analysis , and implementation of a new adaptive chatter control system in internal turning 1637–1659.

Fallah, M., Moetakef-Imani, B., 2017. Analytical Prediction of Stability Lobes for Passively Damped Boring Bars. Journal of Mechanics 1–14. https://doi.org/10.1017/jmech.2017.22

Gonzalez, T., Moreno, J., Fridman, L., 2012. Variable Gain Super-Twisting Sliding Mode Control. IEEE Transactions on Automatic Control 57, 2100–2105.

Hayati, S., Hajaliakbari, M., Rajabi, Y., Rasaee, S., 2018. Chatter reduction in slender boring bar via a tunable holder with variable mass and stiffness. Proceedings of the Institution of Mechanical Engineers, Part B: Journal of Engineering Manufacture 232, 2098–2108. https://doi.org/10.1177/0954405417690554

Kong, L., Chin, J.H., Li, Y., Lu, Y., Li, P., 2014. Targeted suppression of vibration in deep hole drilling using magneto-rheological fluid damper. Journal of Materials Processing Technology 214, 2617–2626. https://doi.org/10.1016/j.jmatprotec.2014.05.029

Kumar, G.P., Seetharamaiah, N., Prasad, B.D., 2017. Improvement of Surface Quality using Magneto-Rheological Fluid (MRF) Boring Bar 13, 29–46.

Lawrance, G., Paul, P.S., Varadarajan, A.S., Raj, S.B., 2019. Suppression of Tool Vibration in Boring Process : A Review. Journal of The Institution of Engineers (India): Series C 100, 1053–1069. https://doi.org/10.1007/s40032-019-00531-z

Lazoglu, I., Atabey, F., Altintas, Y., 2002. Dynamics of boring processes: Part III-time domain modeling. International Journal of Machine Tools and Manufacture 42, 1567–1576.

Liu, H., Wang, J., Luo, Q., 2020. Effect of controllable magnetic field-induced MRF solidification on chatter suppression of thin-walled parts 2881–2890.

Lu, H., Hua, D., Wang, B., Yang, C., Hnydiuk-stefan, A., Królczyk, G., Liu, X., Li, Z., 2021. The Roles of Magnetorheological Fluid in Modern Precision Machining Field : A Review 8, 1–11. https://doi.org/10.3389/fmats.2021.678882

Lu, X., Chen, F., Altintas, Y., 2014. Magnetic actuator for active damping of boring bars. CIRP Annals - Manufacturing Technology 63, 369–372. https://doi.org/10.1016/j.cirp.2014.03.127

Ma, H., Wu, J., Xiong, Z., 2020. Active chatter control in turning processes with input constraint 3737–3751.

Matsubara, A., Maeda, M., Yamaji, I., 2014. Vibration suppression of boring bar by piezoelectric actuators and LR circuit. CIRP Annals - Manufacturing Technology 63, 373–376. https://doi.org/10.1016/j.cirp.2014.03.132

Mei, D., Kong, T., Shih, A.J., Chen, Z., 2009. Magnetorheological fluid-controlled boring bar for chatter suppression. Journal of Materials Processing Technology 209, 1861–1870. https://doi.org/10.1016/j.jmatprotec.2008.04.037

Mei, D., Yao, Z., Kong, T., Chen, Z., 2010. Parameter optimization of time-varying stiffness method for chatter suppression based on magnetorheological fluid-controlled boring bar 1071–1083. https://doi.org/10.1007/s00170-009-2166-9

Miguélez, M.H., Rubio, L., Loya, J.A., Fernández-Sáez, J., 2010. Improvement of chatter stability in boring operations with passive vibration absorbers. International Journal of Mechanical Sciences 52, 1376–1384. https://doi.org/10.1016/j.ijmecsci.2010.07.003

Moetakef-Imani, B., Yussefian, N.Z., 2009. Dynamic simulation of boring process. International Journal of Machine Tools and Manufacture 49, 1096–1103. https://doi.org/10.1016/j.ijmachtools.2009.07.008

Moradi, H., Movahhedy, M.R., Vossoughi, G.R., 2009. Robust control strategy for suppression of regenerative chatter in turning. Journal of Manufacturing Processes 11, 55–65. https://doi.org/10.1016/j.jmapro.2009.06.002

Moradian, H., Abbasi, M.H., Moradi, H., 2019. Adaptive sliding mode control of regenerative chatter and stability improvement in boring manufacturing process with model uncertainties. Proc IMechE Part C: J Mechanical Engineering Science 234, 1171–1181. https://doi.org/10.1177/0954406219889994

Ngatu, G.T., Wereley, N.M., 2007. Viscometric and Sedimentation Characterization of Bidisperse Magnetorheological Fluids 43, 2474–2476.

Ozlu, E., Budak, E., 2007a. Analytical modeling of chatter stability in turning and boring operations - Part I: Model development. Journal of Manufacturing Science and Engineering, Transactions of the ASME 129, 726–732. https://doi.org/10.1115/1.2738118

Ozlu, E., Budak, E., 2007b. Analytical modeling of chatter stability in turning and boring operations - Part II: Experimental verification. Journal of Manufacturing Science and Engineering, Transactions of the ASME 129, 733–739. https://doi.org/10.1115/1.2738119

Prasannavenkadesan, V., Elango, A., Chockalingam, S., 2015. Chatter Suppression in Boring Process Using Passive Damper 9, 1910–1914.

Shtessel, Y., Edwards, C., Fridman, L., Levant, A., 2014. Sliding Mode Control and Observation. Birkhäuser, New York.

Shtessel, Y., Taleb, M., Plestan, F., 2012. Automatica A novel adaptive-gain supertwisting sliding mode controller : Methodology. Automatica 48, 759–769. https://doi.org/10.1016/j.automatica.2012.02.024

Sidpara, A., Jain, V.K., 2013. International Journal of Machine Tools & Manufacture Analysis of forces on the freeform surface in magnetorheological fluid based finishing process. International Journal of Machine Tools and Manufacture 69, 1–10. https://doi.org/10.1016/j.ijmachtools.2013.02.004

Som, A., Kim, D.H., Son, H., 2015. Semiactive Magnetorheological Damper for High Aspect Ratio Boring Process. IEEE/ASME Transactions on Mechatronics 20, 2575–2582. https://doi.org/10.1109/TMECH.2015.2388861

Song, Q., Shi, J., Liu, Z., Wan, Y., Xia, F., 2016. Boring bar with constrained layer damper for improving process stability 1951–1966. https://doi.org/10.1007/s00170-015-7670-5

Suyama, D.I., Diniz, A.E., Pederiva, R., 2016. The use of carbide and particle-damped bars to increase tool overhang in the internal turning of hardened steel. The International Journal of Advanced Manufacturing Technology 2083–2092. https://doi.org/10.1007/s00170-015-8328-z

Takahashi, W., Suzuki, N., Shamoto, E., 2021. Development of a novel boring tool with anisotropic dynamic stiffness to avoid chatter vibration in cutting Part 1 : Design of anisotropic structure to attain infinite dynamic stiffness. Precision Engineering 68, 57–71. https://doi.org/10.1016/j.precisioneng.2020.11.007

Thomas, W., Diniz, A.E., Pederiva, R., Suyama, D.I., De Albuquerque, M. V., 2019. A new type of impact damper with long overhangs in the internal turning of hardened materials. Procedia CIRP 82, 255–260. https://doi.org/10.1016/j.procir.2019.04.147

Tlusty, J., Polacek, M., 1963. The Stability of Machine Tools Against Self Excited Vibrations in Machining, in: The International Research in Production Engineering Conference, Pittsburgh, PA, ASME. New York, pp. 465–474.

Tlusty, J., Polacek, M., 1963. The stability of machine tools against self-excited vibrations in machining, 1963, in: Proceedings of the ASME International. pp. 465–474.

Tran, M., Hwang, S., 2020. applied sciences Design and Simulation of Electromagnetic Linear Actuators for Jet Dispensers.

Venter, G.S., Silva, L.M. do P., Carneiro, M.B., da Silva, M.M., 2017. Passive and active strategies using embedded piezoelectric layers to improve the stability limit in turning/boring operations. International Journal of Advanced Manufacturing Technology 89, 2789–2801. https://doi.org/10.1007/s00170-016-9620-2

Wan, S., Li, X., Su, W., Yuan, J., Hong, J., 2020. Active chatter suppression for milling process with sliding mode control and electromagnetic actuator 136. https://doi.org/10.1016/j.ymssp.2019.106528

Wang, M., Fei, R., 2001. On-line chatter detection and control in boring based on an electrorheological fluid. Mechatronics 11, 779–792. https://doi.org/10.1016/S0957-4158(00)00044-1

Xiong, X., Kamal, S., Jin, S., 2019. Adaptive gains to super-twisting technique for sliding mode design 1–12. https://doi.org/10.1002/asjc.2202

Yao, Z., Mei, D., Chen, Z., 2010. Journal of Materials Processing Technology On-line chatter detection and identification based on wavelet and support vector machine 210, 713–719. https://doi.org/10.1016/j.jmatprotec.2009.11.007

Yigit, U., Cigeroglu, E., Budak, E., 2017. Chatter reduction in boring process by using piezoelectric shunt damping with experimental verification. Mechanical Systems and Signal Processing 94, 312–321. https://doi.org/10.1016/j.ymssp.2017.02.044

Zhu, X., Jing, X., Cheng, L., 2012. Magnetorheological fluid dampers: A review on structure design and analysis. Journal of Intelligent Material Systems and Structures 23, 839–873. https://doi.org/10.1177/1045389X12436735

PUBLICATIONS

Parts of this thesis was published in the following journal articles:

- Saleh MKA, Nejatpour M, Acar HY, Lazoglu I (2021) A new magnetorheological damper for chatter stability of boring tools. J. Mater. Process. Technol. 289:116931–116940. https://doi.org/10.1016/J.JMATPROTEC.2020.116931
- Saleh MKA, Ulasyar A, Lazoglu I (2021) Active damping of chatter in the boring process via variable gain sliding mode control of a magnetorheological damper, CIRP Annals - Manufacturing Technology. https://doi.org/10.1016/j.cirp.2021.04.039